Valence-bond theory of off-center impurities in silicon: Substitutional nitrogen

Peter A. Schultz
Department of Physics, University of Pennsylvania, Philadelphia, Pennsylvania 19104-6396
and Laboratory for Research on the Structure of Matter, University of Pennsylvania, Philadelphia, Pennsylvania 19104-3859

R. P. Messmer
General Electric Company, Corporate Research and Development Center, P.O. Box 8, Schenectady, New York 12301;
Department of Physics, University of Pennsylvania, Philadelphia, Pennsylvania 19104-6396;
and Laboratory for Research on the Structure of Matter, University of Pennsylvania, Philadelphia, Pennsylvania 19104-3859
(Received 19 February 1986)

A theoretical description of the electronic structure of defects in semiconductors is presented that emphasizes the local bonding environment of the defect. For quantitative results, correlated *ab initio* wave functions, within the generalized valence-bond method (GVB), are used in describing defect properties. Explicit, detailed calculations are presented for the example of the substitutional nitrogen defect in silicon. The language of bond pairs, lone pairs, and dangling bonds—concepts well defined within the context of the GVB wave functions used here—is found to be a natural language for the discussion of simple defect behavior. The heretofore obscure driving force for the observed C_{3v} ground-state geometry for $Si{:}N_{Si}$ is revealed to derive from *local* bonding considerations: The nitrogen atom prefers to form only three covalent bonds and have one lone pair, as in ammonia; this naturally results in a C_{3v} ground state. Calculations confirm this description, but the arguments are not dependent on them. The crucial role of electronic correlation, neglected in mean-field approaches, for the description of the character of the local electronic structure of a defect is detailed. Comparisons are made between the results of correlated GVB and mean-field Hartree-Fock calculations which illustrate the importance of electronic correlation effects. The wave functions obtained are then used to calculate the hyperfine coupling parameters, from valence Mulliken analyses and directly from all-electron calculations. Agreement with the very detailed results of electron paramagnetic resonance experiments is quite good and the values obtained are insensitive to minor alterations to the model. The arguments used for the nitrogen-impurity case are not species specific; the behavior of a large class of defects can be qualitatively described by the judicious application of well-established local chemical and physical concepts. A few representative systems are discussed qualitatively to illustrate the usefulness of the simple concepts presented here.

I. INTRODUCTION

The understanding and description of the properties of defects in semiconductors have a long and venerable past.[1] Even with the advent of the ready availability of large-scale computing power, theory still lags far behind experiment in the modern era of semiconductor science. While the reigning paradigm for the description of the electronic structure of a perfect crystal such as silicon is band theory, the breakdown of Bloch's theorem upon the introduction of a defect renders it an inappropriate description in those systems. For those defects which pose only a minor perturbation to the crystal potential, the shallow-level defects with energy levels near the band edges, effective-mass theories[2] have proven to be an adequate description of the electronic states (except for as yet unresolved discrepancies in the description of the ground state where the wave function has its greatest amplitude nearest the defect nucleus[3]). The large body of defects in semiconductors, particularly those of technological and fundamental interest (carrier traps, recombination centers, carrier lifetime control centers), are "deep-level" defects with electronic levels farther from the band edges. It is these defects that have proven the greatest challenge to the theorist.[1] The challenge lies in treating a defect in an otherwise perfect host when the defect potential presents a strong perturbation to the crystal potential and hence the Bloch states are locally a poor basis with which to describe inherently local states. The problem is further complicated by the necessity to consider atomic relaxations that can be energetically significant. The latter effect makes the theoretical definition of an electrical "level" in the gap not such a straightforward issue. Considering the difficulties that need to be surmounted, it is no surprise that a general censenus has yet to emerge on the theoretical treatment of these systems. Recent theoretical investigations of the electronic structure of defects in silicon can be divided roughly into two broad classifications: those that employ cluster methods, stressing the local environment of the defect, and perturbative methods which start with the perfect crystal one-electron band states, usually contained in a perfect-crystal Green's function.

First-principles self-consistent Green's-function calculations have recently enjoyed much acclaim due to the development of the formalism and successful implementation of techniques[4–6] that allow the calculation of total

energetics in defect systems. One application of the method to a study of interstitial aluminum in silicon[5] discussed a possible migration path and proposed a new mechanism to account for the experimentally observed enhanced migration. In another study, Car *et al.*[6] performed a set of calculations on the silicon self-interstitial in an attempt to explain its apparently athermal migration.

To make the calculations tractable, these methods usually employ the local-density approximation[7] (LDA) within density-functional theory.[8] A small cluster of atoms is treated explicitly while the electronic states are coupled to bulk band states by the Green's function. The LDA has been used with success for calculating ground-state properties for such common semiconductors as silicon and germanium.[9,10] The lattice constant is typically reproduced to within 1% of the experimental value, the bulk modulus to within 5—20%, and the cohesive energy to within 15—30%. Recently, however, the inadequacy of the LDA in reproducing the excited-state band structure has come to light,[10–12] the so-called "band-gap problem." Calculations using the LDA consistently underestimate the band-gap energy, typically by 30—50%, so that the silicon LDA gap is approximately half that of experiment[11] while the germanium LDA gap is near zero.[12] Since the ground-state electronic structure of defect systems in Green's-function calculations is intimately dependent on the proper description of the perfect-crystal band states, this shortcoming has serious implications and much effort has been expended in the elucidation of the source of this problem and its possible remedies.[13] One option is simply to rigidly shift the conduction-band-state energies to match the experimental gap through a "scissors operator"[14] before the Green's function is calculated. Although not a panacea, it does allow work to progress on these defect problems until there is a true resolution to the band-gap problem.

The cluster methods attempt to simulate the defect environment by treating a limited number of atoms surrounding the defect. The first of these is the "defect-molecule" calculation of Coulson and Kearsley[15] for the diamond vacancy. They used the sp^3 dangling-bond orbitals of the vacancy to construct a configuration-interaction (CI) calculation to evaluate the lowest-energy states of the neutral vacancy. This first treatment was neither variational nor did it take into account lattice relaxations, but it has served as a good conceptual model for future studies. A more ambitious attempt was that of Messmer and Watkins,[16] who within extended Hückel theory (a parametrized molecular-orbital method) treated the vacancy and the nitrogen substitutional defect in diamond, a system analogous to the subject of the present work, using a large cluster to simulate the defect environment. As in silicon, substitutional nitrogen in diamond is observed to be displaced trigonally from the high-symmetry tetrahedral geometry.[17] The calculation was able to reproduce the proper ground-state geometry, namely a $[\bar{1}\,\bar{1}\,\bar{1}]$ displaced nitrogen, but attributed the cause of the distortion to a Jahn-Teller instability[18] in the calculated degenerate ground state of the tetrahedrally symmetric defect system. Subsequent studies[19–21] determined that the ground state for the high-symmetry T_d defect system is nondegenerate, invalidating the appeal to the Jahn-Teller theorem to account for the existence of a broken-symmetry ground state.

Theoretical models of defect systems use mean-field theory almost exclusively. Hartree-Fock theory and its parametrized derivatives, which by definition include no electronic correlation effects, have been the approximations of choice for cluster methods due to their relative computational simplicity. Only rarely are correlation effects considered, such as in the simple Coulson and Kearsley model[15] or the more sophisticated study of the low-lying covalent states of the neutral silicon vacancy of Surratt and Goddard.[22] Most of the remaining methods employ various local-density approximations in their calculations to account for exchange and correlation. An essential part of such a LDA calculation involves the self-consistent solution of a one-electron Schrödinger equation, the exchange and correlation being included through a one-electron potential. This exchange-correlation potential, dependent on the local electron density, is a mean-field potential.

For these mean-field methods, electrons are distributed pairwise (for non-spin-polarized cases) into usually *delocalized* one-electron orbitals. The delocalization of the orbitals, often dictated by the requirements of symmetry, makes it very difficult to discern the nature of the electronic state, i.e., the nature of the bonding is obscured by the symmetry-required delocalization of the one-electron orbitals and one is frequently left with little more than the symmetry of the state, orbital eigenvalues, and the charge density from which to infer information. Interpretation of the wave function by investigating the forms of the orbitals of such wave functions is usually ignored.

For many years, the concepts of localized bonds in molecules have been found to be extremely useful and powerful tools in the interpretation and prediction of molecular structure.[23] The fundamental principles so useful in understanding molecules should be no less valid when applied to solids and certainly a great deal of insight could be gained from the judicious application of simple chemical and physical concepts. For example, the nature of the driving force for the trigonally distorted ground-state geometry of substitutional nitrogen in diamond or silicon, attributed to either an unspecified strong chemical-rebonding effect in a self-consistent Green's-function study of on-center nitrogen in diamond[20] or to a pseudo-Jahn-Teller effect in a recent molecular-orbital cluster calculation of nitrogen in silicon,[21] is surely due to nitrogen's tendency to form only three bonds and leave two electrons in a lone pair.[24] This viewpoint not only suggests that the nitrogen will distort, but it also predicts the direction of the observed distortion. Computational studies which emphasize energetics and neglect interpretation of the wave function lack this predictive power, and must search the potential energy surface to determine whether a distortion from tetrahedral symmetry will occur and the direction that distortion is likely to take.

Consider the two cases of the nitrogen and oxygen substitutional defects in silicon. Within a one-electron picture, trigonal $\langle 111 \rangle$ and tetragonal $\langle 100 \rangle$ symmetry-

lowering distortions need to be considered on an equal footing for both cases; there are no *a priori* theoretical grounds for the preference of one over the other. Nitrogen is observed to distort trigonally[25] from the tetrahedral geometry while oxygen has a ground-state geometry tetragonally distorted from the tetrahedral geometry.[26,27] After investigating both possible distortion modes, the molecular-orbital (MO) theory is able to reproduce the correct behavior for both the nitrogen and oxygen defect systems,[21] *but is unable to explain why the two cases should be different.* What appears to be a mystery when viewed from conventional one-electron approaches emerges from a more bond-oriented picture (rather than MO or band-oriented) to be a natural consequence of the chemical nature of the impurities involved: oxygen will form two bonds instead of three and will move off in a ⟨100⟩ direction so as to accommodate this tendency. This point is elaborated upon in later sections.

The approach that we apply to address the deep-level defect problem is the perfect-pairing form of the generalized valence-bond (GVB-PP) method.[28] The GVB-PP method is an *ab initio* approach in which the forms of the orbitals are obtained from fully-self-consistent calculations. It goes beyond mean-field theory to include electronic correlation (many-body effects) in a systematic and well-defined fashion. The incorporation of correlation into the calculation proves very important in the qualitative interpretation of the resulting wave function and may lead to qualitative differences in the physics obtained from the calculations.

Unlike the doubly occupied delocalized orbitals that result from mean-field calculations, the incorporation of correlation in the GVB-PP calculation variationally causes the GVB-PP orbitals to localize into structures readily identified as bond pairs, lone pairs, and dangling bonds, concepts ill defined in a mean-field theory. In mean-field theories, any unitary transformation of the occupied orbitals, changing their shape and therefore the description of the bonding, leaves the energy invariant. In this correlated theory the forms of the orbitals are variationally determined using an energetic criterion; changing their shapes will change the energy. This allows for a unique interpretation of the wave function not possible in an uncorrelated mean-field approach. The qualitative difference in the resulting wave functions results from the incorporation of correlation. The predictive power afforded by such an analysis of the wave function makes this method ideally suited to the description of a large class of defect systems such as those mentioned above.

The purpose of this paper will be twofold: First, to illustrate the usefulness of this conceptual viewpoint and secondly to present a detailed application to a particular example, the nitrogen substitutional defect in silicon, using a method that captures the essential features needed to make contact with that viewpoint. The outline of the remainder of the paper is as follows. In the next section we provide the computational details of the calculations. Section III will expand on the nature of the GVB-PP wave function and its properties in order to make more familiar the concepts crucial to the development of the arguments we present. The method we apply requires the use of a cluster approximation. Given the obviously important limitation of not treating the host lattice explicitly, we devote Sec. IV to the justification of the validity of the cluster approach, the development of the particular cluster model we use, and the tests of how well the cluster model chosen reproduces bulk characteristics. The results obtained are compared with alternative cluster-termination methods suggested by other investigators. The results for substitutional nitrogen in silicon are presented in Sec. V. The discussion of Sec. VI reviews the results, discusses the generalization of the method to other defect systems, and assesses the benefits and the limitations of the current approach. We present our conclusions in Sec. VII.

II. COMPUTATIONAL DETAILS

A. Cluster model

The model used to represent the local environment of bulk silicon is a $Si_5H^x_{12}$ cluster, depicted in Fig. 1. It consists of the central silicon, its four tetrahedral nearest-neighbor silicon atoms, and a set of twelve terminating atoms to saturate the dangling bonds. The terminating "H^x" atoms are hydrogen atoms with basis sets (Sec. II C) specially modified to simulate the presence of the absent host crystal. Our defect models then simply involve replacing the central silicon atom with the desired impurity, e.g., the substitutional nitrogen defect is modeled by a $NSi_4H^x_{12}$ cluster. The Si-Si separation used is 2.35 Å with the H^x located 1.73 Å from the silicon atoms for all but the calculations which study the effect of nitrogen displacement in a rigid cage. In that case, the Si-H^x distance used is 1.50 Å.

B. Wave functions

All the calculations employ *ab initio* methods in which the forms of all the orbitals are solved for self-

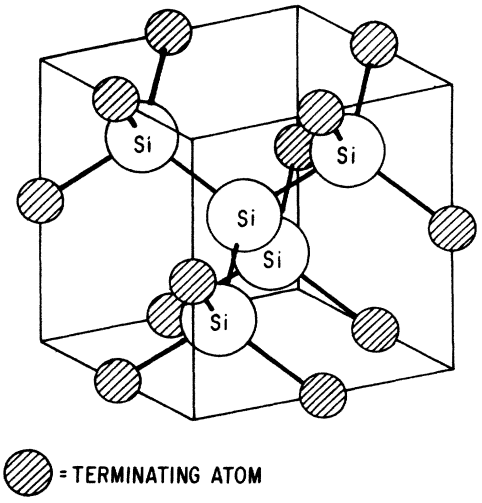

FIG. 1. The $Si_5H^x_{12}$ cluster used to simulate the environment about a single lattice site.

consistently. The ten core electrons ($1s^2 2s^2 2p^6$) of the silicon and phosphorus atoms are replaced by effective potentials[29] (*ab initio* pseudopotentials), except in those cases where hyperfine calculations require detailed information about the wave function near the nucleus; in such cases the core electrons are included in an all-electron calculation. The results presented include Hartree-Fock (HF) and GVB perfect-pairing calculations.[28] For substitutional nitrogen, the self-consistent solution of the GVB equations yield wave functions of symmetry lower than the nuclear Hamiltonian. For fully quantitative results in this event, a total wave function having the proper symmetry is constructed by taking a linear combination of the broken symmetry GVB-PP solutions. This approach of mixing nonorthogonal wave functions was first applied in the case of molecular systems and called the resonating generalized valence-bond method (R-GVB),[30] so labeled because it represents the theoretical embodiment of the chemical idea of resonance. These wave functions will be referred to as R-PP below in order to be more specific about the component wave functions of the total wave function.

For the familiar case of the HF (or MO) wave function, the electrons are distributed in a pairwise manner into orthogonal one-electron orbitals ϕ_i such that the resulting wave function can be written as a single Slater determinant. The HF wave function for the defect cluster described above, with either 32 or possibly 33 valence electrons, can be written as

$$\Psi_{\mathrm{HF}}=\mathscr{A}[\Phi_1(1,2)\cdots\Phi_{16}(31,32)\phi_e(33)\alpha(33)] , \quad (1)$$

where $\mathscr{A}$ is the antisymmetrization operator and

$$\Phi_i(2i-1,2i)=\phi_i(2i-1)\phi_i(2i)\alpha(2i-1)\beta(2i) . \quad (2)$$

This is the simplest form of wave function used in this study.

Within the perfect-pairing form of generalized valence-bond theory, the restriction that two electrons be placed in one orbital is lifted. The form of the wave function Ψ_{PP} (we will use the labels GVB-PP and PP interchangeably) is similar to that of Ψ_{HF} in Eq. (1), except that each of the two electrons in a pair are allowed to have their own orbital (neglecting normalization):

$$\Phi_i=[\psi_{i,1}(1)\psi_{i,2}(2)+\psi_{i,2}(1)\psi_{i,1}(2)]\alpha(1)\beta(2) , \quad (3)$$

where the perfect-pairing orbitals $\psi_{i,1}$ and $\psi_{i,2}$ overlap and are coupled into a singlet spin state. The special case in which the spatial functions $\psi_{i,1}$ and $\psi_{i,2}$ are forced to have unit overlap is a possible solution for this wave function; in this case Eq. (3) reduces to Eq. (2) and the HF result is obtained. Ordinarily, though, the two electrons take advantage of the additional variational flexibility to "correlate" their motions and thereby reduce the repulsions between them.

The orbitals of the GVB-PP calculation, overlapping within pairs, are kept orthogonal between pairs (the "strong-orthogonality" constraint). Computationally, it is more convenient to transform the PP orbitals into an orthogonal natural orbital representation:

$$\begin{aligned}\psi_{i,1}(1)\psi_{i,2}(2)+\psi_{i,2}(1)\psi_{i,1}(2)&=\tfrac{1}{2}\{[\lambda_{i,b}\phi_{i,b}(1)+\lambda_{i,a}\phi_{i,a}(1)][\lambda_{i,b}\phi_{i,b}(2)-\lambda_{i,a}\phi_{i,a}(2)]+(1)\leftrightarrow(2)\}\\&=\lambda_{i,b}^2\phi_{i,b}(1)\phi_{i,b}(2)-\lambda_{i,a}^2\phi_{i,a}(1)\phi_{i,a}(2) ,\end{aligned} \quad (4)$$

where $\phi_{i,b}$ and $\phi_{i,a}$ (the natural orbitals of pair i) are now orthogonal to each other (and to all other natural orbitals). A GVB-PP wave function with N pairs can be written as a product of N of these terms in a CI expansion. Hence, the calculation is a self-consistent multiconfiguration calculation with 2^N configurations. Mean-field calculations consist of only one configuration and assign pairs of electrons to particular orthogonal orbitals. While formally a multiconfigurational method, GVB-PP also retains a single-particle interpretation within the nonorthogonal PP orbital representation of Eq. (3) or (4), where one electron is assigned to each orbital.

For the cluster calculations, two levels of perfect-pairing correlation were used: those in which all 16 pairs of valence electrons were correlated using $16\times 2=32$ natural orbitals, denoted PP(16/32), and a simpler wave function, denoted PP(4/8), which correlates only the four pairs of electrons (with two natural orbitals each) that have self-consistently localized into orbitals that can be associated with the four pairs of electrons about the nitrogen. The 24 silicon-terminator bond electrons are treated at the Hartree-Fock level in this situation. For varying geometries, the PP(4/8) results gave approximately the same relative energies as the PP(16/32) results. Thus, for computational simplicity, the PP(4/8) wave function is the one primarily used.

From the R-PP calculations, we obtain the total wave function

$$\Psi_{\text{R-PP}}=\sum_I c_I\Psi_{\mathrm{PP},I} \quad (5)$$

from the perfect-pairing wave functions Ψ_I (dropping the PP label) by solving the secular equation $\det|\underline{H}-E\underline{S}|=0$, where $H_{IJ}=\langle\Psi_I|H|\Psi_J\rangle$ and $S_{IJ}=\langle\Psi_I|\Psi_J\rangle$ gives the overlap matrix. Since the wave functions Ψ_I are, in general, nonorthogonal, this is a nontrivial calculation and therefore only the coefficients c_I are solved for, i.e., the orbitals of the Ψ_I are not reoptimized. In a sense, this may be thought of as simply a CI among nonorthogonal basis states. Such a calculation was performed for the broken-symmetry PP solutions for the nitrogen impurity cluster. Again, for computational simplicity, only the PP(4/8) wave functions were used as the basis states for this calculation, resulting in R-PP(4/8) wave functions.

C. Basis sets

Standard valence double-zeta (VDZ) or full double-zeta (DZ) Gaussian basis sets[31] were used on all atoms. The terminating H^x-atom basis function consisted of three s Gaussians contracted into a single Slater-function-simulating function,[31(a)] denoted $(3s/1s)$, with a scale factor of 0.5154. For the nitrogen atom we used a $(9s\,5p/3s\,2p)$ VDZ basis set[31(b)] in a majority of the calculations and a $(9s\,5p/4s\,2p)$ DZ basis set[31(c)] to better describe the Fermi contact term in the hyperfine calculations. The silicon and phosphorus cores were usually replaced by effective potentials and a $(3s\,3p/2s\,2p)$ basis used to describe the valence electrons.[29] In the cases where it was necessary to treat the core electrons explicitly, a DZ $(11s\,7p/6s\,4p)$ basis set was used.[31(b)] For real hydrogen atoms, a $(5s/2s)$ basis set[31(b)] with a scale factor of 1.2 was used. In some calculations, basis functions of higher-angular-momentum (polarization functions) or more diffuse Rydberg functions were added to the basis set. They consisted of single Gaussians; the type of function and the values of their exponents are presented in Table I.

III. THE NATURE OF THE CORRELATED WAVE FUNCTION

What distinguishes the current approach from most previous impurity and defect studies in semiconductors is the explicit inclusion of electronic correlation (many-body) effects. The only previous attempts to incorporate correlation effects have involved simple models such as the defect molecule of Coulson and Kearsley. The GVB method, however, has been applied with considerable success to semiconductor surface problems.[32–35] Although Surratt and Goddard[22] applied a related CI method to the silicon vacancy, such an approach was not pursued further for bulk defect studies. The current study is the first that attempts to present a correlated wave-function approach to treat point defects in general. A simple example of the properties of a perfect-pairing wave function will clarify the principles which will be used later.

A. The hydrogen molecule and a bonding pair of electrons

The simplest system for discussing the effect of correlating a pair of electrons is the hydrogen molecule. In the MO wave function Ψ_{MO}, two electrons are placed in the bonding orbital ϕ_b, one spin up (α) and one spin down (β):

$$\Psi_{HF}=\mathcal{A}[\phi_b^2\alpha\beta]\ , \tag{6}$$

while in the perfect-pairing wave function, each electron occupies its own orbital:

$$\Psi_{PP}=\mathcal{A}[(\psi_l^1\psi_r^1)(\alpha\beta-\beta\alpha)]$$
$$=\mathcal{A}[(\psi_l^1\psi_r^1+\psi_r^1\psi_l^1)(\alpha\beta)]\ . \tag{7}$$

Using a single-zeta basis, Fig. 2(a) presents the resulting H-H binding curves for the two wave functions, Ψ_{HF} [Eq. (6)] and Ψ_{PP} [Eq. (7)], as a function of internuclear separation. Note that as the internuclear distance increases, the difference in energy of the two methods increases, as shown in Fig. 2(b). The PP wave function dissociates to the correct limit while the HF one does not. The source of the error is well known and is simply illustrated by viewing the orbitals generated by the HF and PP wave functions as the atoms are separated (Fig. 3). Figure 3(a) presents the contour plots of the Hartree-Fock one-electron orbital ϕ_b, seen to delocalize onto both atoms at all separations. The contour plots of Figs. 3(b) and 3(c) show the two PP bond orbitals ψ_l and ψ_r of the PP wave function and demonstrate that this PP wave function approaches the correct bond-dissociation limit, H^0+H^0, of noninteracting atoms as infinite separation is approached. One orbital, ψ_l, localizes predominantly on the left-hand atom, while the other orbital, ψ_r, localizes predominantly on the right-hand atom. This allows us to use the valence-bond diagram of Fig. 3(d) to schematically represent the PP wave function for the hydrogen molecule.

B. Localization and transferability of orbital pairs

The added computational complexity of the GVB-PP is offset by the conceptual advantages gained from the use of the localized orbitals that result from the inclusion of electronic correlation in the wave functions. Take, for example, the case of the ammonia molecule. Intuitively, one expects to see three nitrogen-hydrogen bonds and a nitro-

TABLE I. Basis-function exponents for polarization and Rydberg functions.

	Basis-function type		
	Polarization	Rydberg	
Atom	d	s	p
N	0.8	0.028	0.025
Si	0.3247	0.017	0.014
P		0.020	0.027

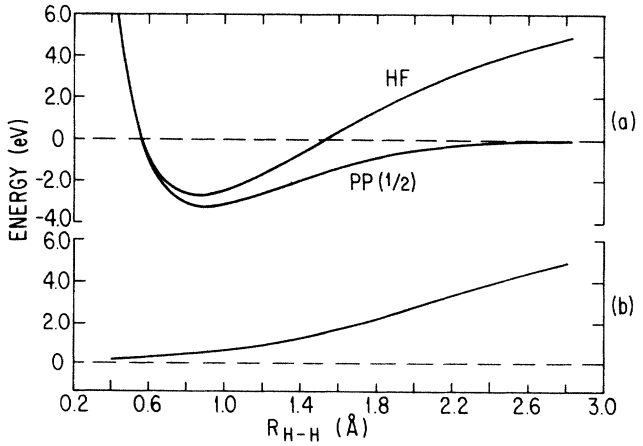

FIG. 2. Energy curves for a H—H bond using a simple single s basis function on each atom. (a) Bonding curves for the Hartree-Fock and GVB perfect-pairing wave function. (b) The difference of the two results, illustrating that the correlation error in a bond increases with increasing separation.

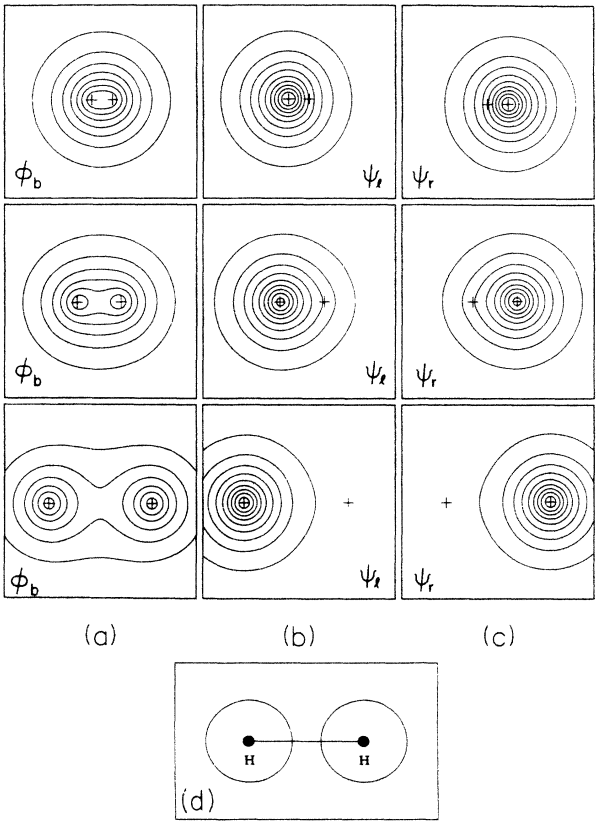

FIG. 3. The contour plots of the orbitals of the self-consistent Hartree-Fock and perfect-pairing wave functions at three successive distances: 0.40, 0.85, and 2.00 Å. (a) ϕ_b of the Hartree-Fock wave function; doubly occupied. (b) and (c) ψ_l and ψ_r of the perfect-pairing wave function. Each is occupied by a single electron and the two are singlet coupled. (d) Schematic depiction of the perfect-pairing wave function.

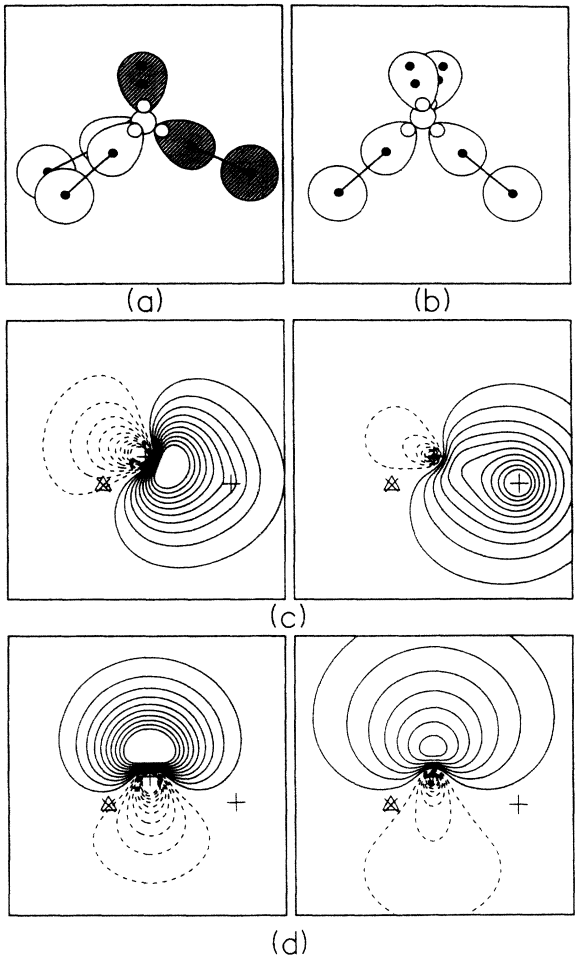

FIG. 4. Valence-bond representation of simple molecules. (a) The schematic depiction of a perfect-pairing wave function for ammonia. The shaded orbitals are plotted in (c) and (d). (b) The schematic depiction of the perfect-pairing wave function of the water molecule. Two lone pairs (not shown) which resemble the lone-pair orbitals of (c) and two O—H bonds [resembling the N—H orbitals of (b)] result from the perfect-pairing calculation. (c) The two perfect-pairing orbitals of one of the three symmetrically related nitrogen-hydrogen bond pairs of a self-consistent PP(4/8) wave function. The other two bond pairs are obtained by a C_3 rotation about the z axis (vertical). (d) The in-out correlated lone pair of the same wave function.

gen lone pair, as shown by the valence-bond diagram of Fig. 4(a). For the perfect-pairing calculation, there are four pairs of valence electrons which can be correlated to obtain a PP(4/8) wave function. Upon calculation, the PP orbitals localize and three pairs describing three equivalent N—H bonds result, a representative one being shown in Fig. 4(c), and the single lone pair of Fig. 4(d) emerges. The wave function has self-consistently adopted the form represented by Fig. 4(a), as valence-bond ideas would suggest, though it is not *a priori* required that this be the case. There is often a one-to-one correspondence between the GVB-PP wave function for a system and a simple valence-bond diagram. Extending this picture to the water molecule, one expects to find two bonds to hydrogen atoms and two lone pairs as in the depiction of Fig. 4(b). The self-consistent PP(4/8) calculation produces orbitals (not shown) that indeed represent a one-to-one correspondence with the valence-bond diagram. The orbitals of the lone pairs of H_2O resemble those of the single lone pair of NH_3 and the O—H bond-pair orbitals resemble their counterparts in NH_3, though perhaps they are more polarized. The qualitative description of the bonds is transferable between these systems.

The transferability of bonds and bonding behavior will play a key role in the arguments we will make below, but first we will illustrate how it can be useful in the development of a model of the silicon lattice. Consider the sequence of model systems SiH^x_4, $Si_2H^x_6$, and $Si(SiH^x_3)_4$. The "hydrogen" atoms H^x used are our specially modified terminators, located 1.73 Å from silicon atoms. Progressively, we include more and more silicon atoms in the diamond structure and correlate each pair of valence electrons. The three systems have different numbers of atoms and electrons, and belong to two different point-group symmetries. The canonical orbitals that result from a mean-field calculation (HF, MO, or any one-electron calculation) will show little if any resemblance among the

three systems. This is due to the tendency of these orbitals to delocalize over the entire system, compatible with the molecular symmetry. The PP orbitals of the three systems, on the other hand, bear a striking resemblance to one another. The orbital contour plots of selected orbitals of these systems can be found in Fig. 5. For the SiH^x_4 moiety, we obtain four equivalent silicon-terminator bonds. The disilane-analog PP(7/14) calculation produces six equivalent silicon-terminator bonds and a silicon-silicon bond. The last system produces four equivalent Si—Si bond pairs and twelve Si—H^x bond pairs in a PP(16/32) calculation. The Si—Si bond-pair orbitals of $Si_2H^x_6$ and $Si_5H^x_{12}$ (see Fig. 5) are very much alike, even though in one case the silicon atoms are coordinated with three terminator atoms, while in the other case one silicon atom is coordinated with three other silicon atoms. This similarity results because of the very similar environments which the electrons of these two bonds experience. The silicon atoms are all fourfold coordinated into covalent bonds. Hence, it is only natural to expect that the form of the localized bond orbitals of two Si—Si bonds should resemble one another. The Si—H^x bond orbitals of all three systems are also almost identical to each other, the orbitals for the two larger systems being shown in Fig. 5. What is more surprising at first glance is the degree to which the silicon-terminator bond orbitals resemble the silicon-silicon bond orbitals, particularly near the silicon atom. However, given that the H^x's have been modified to simulate silicon atoms, this is perhaps not too surprising after all, but further serves to confirm the approach (described below) which determined the terminators. That these bond orbitals seem almost perfectly transferable between these systems indicates that the local behavior and properties of these localized bonds should also be transferable.

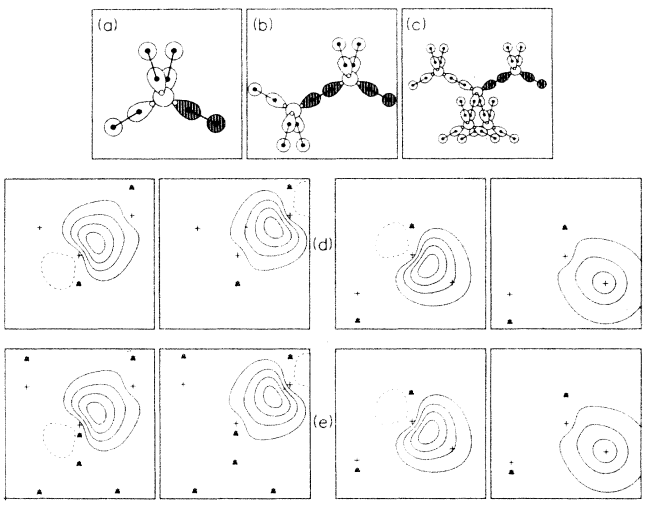

FIG. 5. Illustration of the transferability of bond pairs between different systems that have similar local environments. Considered are the perfect-pairing orbitals of three different clusters: (a) SiH^x_4, (b) $Si_2H^x_6$, and (c) $Si_5H^x_{12}$. The schematic diagrams serve as a summary of the basic features of the many-electron wave function. (d) Contour plots of the Si—Si and Si—H^x bond orbitals for the $Si_2H^x_6$ system, shown as the shaded orbitals of (b). (e) Contour plots of the Si—Si and Si—H^x bond orbitals for the $Si_5H^x_{12}$ system, the shaded orbitals of (c). We note that the Si—Si bond orbitals of the two systems are very similar, as are Si—H^x bond orbitals for all three systems [the orbitals of (a) are not shown].

That the transferability of bonds and bond properties is not just idle speculation is supported by drawing on thermochemical data to compare bond energies in the limits of bulk and molecular systems. The experimental binding energy of the silicon lattice amounts to 4.68 eV/unit cell or 2.34 eV/bond.[36] The heats of atomization of silane and disilane are 13.18 and 21.79 eV, respectively.[36] The first figure implies 3.29 eV/Si—H bond, and subtracting six of these from the second figure (six Si—H bonds) leads to a Si—Si bond energy of 2.02 eV, or only $\sim$0.3 eV/bond different from that of bulk silicon. Table II presents the results of analogous arithmetic for a few elemental tetrahedral semiconductors. The energy of formation of diamond, bulk silicon, and bulk germanium are all rather well approximated. If instead of using thermodynamic data to estimate[37] the $H_3C—CH_3$ bond strength, spectroscopic information pertaining to H_3C-CH_3 dissociation is used to obtain the bond strength, the agreement between the bulk bond energy and the molecular bond energy becomes even more pronounced. While the cohesive energy of the diamond lattice implies a C—C bond energy of 3.67 eV/bond, the spectroscopic dissociation of ethane into two CH_3 fragments yields a C—C bond energy of 3.64 eV.[38]

The bond energy is not the only characteristic of bonds that is common between the bulk and molecules. The energy of stretching those bonds is similar in the bulk and the respective H_3X-XH_3 molecules. The X-X force constant from the H_3X-XH_3 molecules and the values derived from the bulk moduli for diamond, silicon, and germanium[39] agree to within 7—25%. The lattice constants for diamond, silicon, and germanium[39] can also be approximated quite well (to within 1—2%) by using the values for X—X bond distances in the respective H_3X-XH_3 molecules.[38] In the case of silicon, estimates of the bulk ground-state lattice constant, bond force constant, and cohesive energy can be obtained with an accuracy of 1%, 7%, and 14%, respectively, by using values taken from the H_3Si-SiH_3 molecule. Thus, the properties of these local bonds do appear to be transferable between different systems. We will take advantage of this transferability of bonds and bond characteristics, demonstrated by this analysis, to develop our model for the bulk and defect systems.

TABLE II. Comparison of bulk and molecular bond energies (eV) for simple semiconductors.

Element	Carbon	Silicon	Germanium
Lattice bond	3.67	2.34	1.94
H_3X—XH_3 bond	3.36 (3.56[a])	2.02	1.83

[a] Bond energy when hydrogens are replaced by chlorines.

IV. THE CLUSTER APPROXIMATION

A. Qualitative discussion

The similarity of orbitals among different systems discussed above is a consequence of the similarity of the local environments. Thus, the PP wave function for the $Si(SiH^x_3)_4$ cluster can be qualitatively described in terms of the orbitals of the PP wave function for the $Si_2H^x_6$ cluster. Extrapolating from the SiH^x_4, $Si_2H^x_6$, $Si_5H^x_{12}$ sequence through progressively larger structures, the electronic ground state for a tetrahedral semiconductor such as silicon would be well described by a many-electron wave function consisting of localized correlated valence-bond orbitals between neighboring silicon atoms, much like the bond orbitals associated with the silicon-silicon bonds described above. It was Slater[40] who first suggested that such an approach would be appropriate for the description of the electronic structure of a covalent solid such as silicon. The formalism for just such a description of an infinite solid by a multiconfigurational method such as GVB within the perfect-pairing approximation has been developed,[41] but has yet to be implemented. The hypothetical infinite solid many-electron wave function, concentrating on the local vicinity of the silicon atom in Fig. 1, can be written as

$$\Psi_{\text{bulk}}=\mathscr{A}[\cdots\Phi_A\Phi_B\Phi_C\Phi_D\cdots], \tag{8}$$

where the perfect-pairing orbitals ψ_{A1} and ψ_{A2} of Φ_A correspond to the two orbitals which make up the localized covalent single bond from the central silicon atom to a neighboring silicon atom.

There exists a fundamental difference in the outlook between a mean-field description and a correlated electron approach such as the generalized valence-bond theory description of the solid. The conventional mean-field approach takes the one-electron band states as the primary focus in the discussion of solid-state electronic structure and bonds are, at best, inferred. In a correlated wave-function approach such as valence-bond theory the bonds of the solid are the primary focus and the bands are inferred. It is not necessary within this approach to reproduce the band structure in order to achieve a proper description of the ground state of a semiconductor. In a correlated approach such as the GVB-PP, which results in localized overlapping bond orbitals between neighboring atoms, the total wave function for the system, Eq. (8), has all the physically required symmetry properties, i.e., *the individual electronic orbitals need not satisfy Bloch's theorem.* The customary use of the Bloch states in the description of the *ground state* is a mathematical by-product of the mean-field approximation and is not an essential part of the physics. A discussion of the treatment of the excited states of the solid from the local bond viewpoint, i.e., the determination of the band structure will be presented elsewhere.[42] We merely note here that the nature of these excited states is rather different than that of the ground state.

The challenge is to model the environment about a single site and an important question inherent to any cluster approach is how to terminate the cluster so as to accomplish this. Within the GVB-PP, the valence electrons of the infinite solid ground state are represented by the localized orbitals of the many-electron wave function of Eq. (8). Consider the PP cluster wave function

$$\Psi_{\text{cluster}}=\mathscr{A}[\Phi_{\text{tr}}\Phi'_A\Phi'_B\Phi'_C\Phi'_D], \tag{9}$$

such that the orbitals of $\Phi'_A-\Phi'_D$ are the Si—Si bonds about the central silicon atom and Φ_{tr} takes account of the orbitals involved in truncation of the cluster. Encouraged by the near universality of bond properties illustrated in the analysis above, we strive to reproduce the local electronic structure about one lattice site, i.e., the object is to develop a cluster termination such that orbitals of $\Phi'_A-\Phi'_D$ in the cluster wave function [Eq. (9)] take the same form as the orbitals of $\Phi_A-\Phi_D$ in the bulk [Eq. (8)]. Within this framework lies a justification for the use of the cluster approximation, a justification more difficult to rationalize from a mean-field framework. The perfect-crystal mean-field wave functions involve maximally delocalized one-electron Bloch states that nominally make no contact with the cluster mean-field one-electron states. The criteria for the quality of the reproduction of the local environment by the cluster calculation are unclear. The local nature of the PP orbitals in the ground state for the bulk and cluster wave functions makes direct contact between bulk and cluster possible. It does not require reproducing the entire band structure; instead, one is concerned only with describing the local ground-state electronic structure about the defect of interest, which will be very similar in the solid and in a cluster.

The PP orbitals, if the cluster is well designed, will bear a direct resemblance to their counterparts in the infinite solid wave function. The electronic structure of the system upon the introduction of a point defect should be well modeled by this procedure, especially when the electrons associated with the defect are very localized in nature, as is often the case, as demonstrated by electron paramagnetic resonance (EPR). Examples include such impurities as substitutional oxygen and the case we consider in detail: substitutional nitrogen in silicon.

B. Quantitative analysis

To obtain a reasonable description of the properties of a defect in silicon by modeling the infinite solid by a finite cluster requires that the treatment of the surface of that cluster be done with care. A common approach in cluster methods is to include as many bulk atoms as possible and to tie off the dangling bonds with hydrogen atoms. The model we adopt for our study is the $XSi_4H^x_{12}$ cluster. There have been numerous approaches to terminating this sort of cluster: with the hydrogen atoms at Si-H equilibrium distance, 1.48 Å, or at "bulk" separation, 2.35 Å, or at some suitable compromise in between. One of the most prominent drawbacks associated with this stratagem derives from hydrogen being more electronegative than silicon, leading to a skewed electron distribution. A recent twist is to modify the hydrogen basis set so that the electronegativities of the specially modified hydrogen atoms (MHA's) and the silicon atoms they model are approximately the same.[32] This approach was first applied

by Redondo *et al.* in the study of the oxidation of silicon surfaces.[32] Using a single-zeta basis set, $\xi=0.2944$, on the terminating MHA and placing them at silicon bulk positions, a self-consistent calculation for a terminated Si_5 cluster results in an electron distribution that leaves the central silicon atom approximately neutral. We have adopted a strategy similar in spirit though different in detail for the development of our cluster model.

A nearly ideal electron distribution, within 0.1% of four valence electrons per silicon in a Mulliken analysis,[43] was obtained in a PP(16/32) calculation for the $Si_5H^x_{12}$ cluster using terminating hydrogen atoms with single-zeta basis sets, $\xi=0.5154$, located 1.5 Å from the silicon atoms. If possible, however, it is advisable to have terminating atoms at equilibrium distances to avoid some difficulties associated with how to treat atomic relaxations upon the introduction of a defect. Optimal bond distances were calculated with varying levels of correlation included in the wave function. The optimal silicon-silicon distance for the silicon cluster model $Si_5H^x_{12}$ using a PP(16/32) wave function was 2.345 Å, while the silicon-terminator distance was optimal at 1.755 Å. Correlating only the Si—Si bond-pair electrons (treating the electrons associated with the silicon-terminator bonds at the HF level) results in a slightly longer Si—Si bond (2.35 Å), while the Si-H^x distance decreases to 1.73 Å. The cluster optimization using a Hartree-Fock wave function yields a Si-H^x distance of 1.727 Å and a moderately shortened silicon-silicon bond distance of 2.326 Å.[44] The PP(4/8) is the wave function used in the geometry optimizations in the nitrogen defect system; hence the model chosen for those calculations had the terminators located 1.73 Å from the silicon atoms.

In using this cluster ($R_{\text{Si-H}^x}=1.73$ Å instead of 1.50 Å) the electron distribution for the PP(16/32) wave function has deviated from ideal by only 1% (see Table III), which is more than adequate considering the imprecise nature of the Mulliken analysis. The bond-stretch force constant for a correlated Si—Si bond is calculated to be 10.1—10.5 eV/Å^2, depending on the cluster and whether neighboring bonds are correlated also. This is in good agreement with the corresponding bulk value[39] of $\sim$10.2 eV/Å^2. The value for an uncorrelated Si—Si bond is 20% higher. The silicon-terminator bonds reproduce rather well the silicon-silicon bonding which they are supposed to simulate. Figure 6 illustrates this with a plot of the energy curves of a typical correlated Si—Si bond with an uncorrelated Si—H^x bond. The fact that the silicon-terminator curve is shallower is reflected in a weaker force constant of 8.5 eV/Å^2. For our full geometry optimizations of the nitrogen defect geometry, we opt to keep the terminators fixed at the PP(4/8) equilibrium position in the $Si_5H^x_{12}$ cluster while allowing the five inner atoms to relax. This relieves us of the need to choose another, perhaps more arbitrary, procedure dealing with the terminating atoms. The weaker Si—H^x force constant can be rationalized as accounting for the effect of more distant bulk atoms relaxing in response to the motion of the atoms free to move in the cluster.

We calculate a cluster "valence-band width" of $\sim$12.2 eV, the more bound state being *s*-like in character, the less bound being *p*-like. Although we cannot expect a finite-cluster calculation to reproduce the absolute values of the bulk ionizations, the fact that the results are consistent with the bulk Γ-point width of 12.5 eV (Ref. 45) is very encouraging.

The development of a new method of termination was motivated by the previously stated desire to reproduce bulk properties as well as possible. Toward this goal, we critically examined several options that had been used in other studies. Table III provides a summary of a few simple properties calculated for clusters terminated with (a) hydrogen atoms at 1.48 Å (Si—H equilibrium bond distance) and 2.35 Å (silicon bulk position), (b) with special terminating MHA's (Ref. 32) located at silicon bulk positions, and (c) our choice of terminators.

TABLE III. Silicon Si_5A_{12} cluster models: Mulliken populations. Population in terms of valence electrons: neutral silicon will have a population of 4.0.

Terminating atom (A)	$R_{\text{Si-}A}$ (Å)	Wave function	Mulliken populations: Central silicon	First-shell silicon	Terminating atom	Si—Si bond dipole moments[a]
Ideal			4.0	4.0	1.0	0.0
Hydrogen[b]	2.35	PP(16/32)	4.19	4.25	0.90	−1.11
	1.48	PP(16/32)	4.47	3.73	1.05	+0.46
MHA	2.35	PP(16/32)	4.01	4.82	0.73	+0.12
		PP(4/8)	3.93	4.90	0.71	
This study H^x	1.50	PP(16/32)	4.00	4.00	1.00	−0.38
	1.73	PP(16/32)	4.05	4.03	0.98	+0.01
		PP(4/8)	4.01	4.10	0.97	
		HF	4.06	4.09	0.97	

[a] In units of debye, directed from the central silicon of the cluster toward the ⟨111⟩ silicon. Calculation is for the two electrons in this bond, about the midpoint of this bond.
[b] Scaled zeta = 1.2.

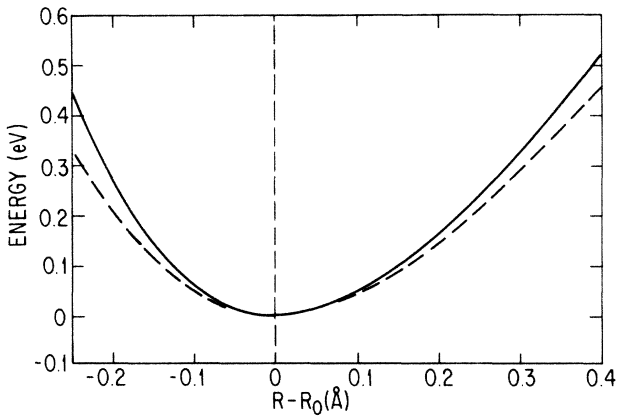

FIG. 6. The potential curves for a typical Si—Si bond [from the PP(7/14) calculation for $Si_2H^x{}_6$] and Si—H^x bond (taken from a HF calculation for $SiH^x{}_4$) to illustrate how the terminator bond behaves in comparison to the silicon-silicon bond that it models.

The use of hydrogen atoms at either bulk or equilibrium positions results in Mulliken populations which are highly unbalanced, due to the differences in electronegativity. Replacing the hydrogens with the special terminating MHA's gives an excellent electron population for the central silicon atom, but less satisfactory values for the nearest neighbors. The populations derived from the fully-self-consistent calculations using our new terminators do rather well in comparison to the other options we considered. This result might have been anticipated from inspecting the almost perfectly symmetric forms of the orbitals of Fig. 5 from the cluster using the new terminators. The Mulliken population is one means of judging the quality of the termination, but the local orbital description provides yet another measure. The electronic dipole of the two electrons of a single bond about the bond midpoint should be zero by symmetry, in the ideal case. The calculated bond dipole moments for a silicon-silicon bond pair using the various clusters are listed in Table III. The new terminators fair quite well by this measure, also. The real hydrogen-terminated clusters have bond dipoles which indicate that the local environments are not being very well reproduced. The Si—Si bond-dipole result using MHA terminators seems to indicate that the Mulliken analysis may be unduly maligning the actual efficacy of this termination. The result using the new terminating atoms is very good.

The cluster model developed here measures up very well to a number of criteria and appears to reproduce the local environment about a silicon atom very well. The overall quality of the results demonstrate that it is not necessary to reproduce the excited-state band structure to obtain a valid description of the local ground-state environment of a single site in the lattice. The formal justification for this strategy provided above is supported by the analyses which verify that the Mulliken populations, lattice constant, bond-stretch force constant, bond-dipole moment, and a valence-band width calculated for the cluster all closely approximate the values in the bulk. We are now ready to address the defect problem.

V. SUBSTITUTIONAL NITROGEN IN SILICON

A. Qualitative discussion

The simple nitrogen substitutional defect has been identified through EPR experiments by Brower.[25] The neutral defect exhibits a C_{3v} symmetry with the unpaired electron localized primarily on a single silicon atom with some small amplitude on the nitrogen atom. According to his analysis, the wave function for the extra electron, ϕ_e, is approximated by a simple LCAO molecular orbital:

$$\phi_e = \sum_i \eta_i(\alpha_i \psi_{i,ns} + \beta_i \psi_{i,np}) , \tag{10}$$

summing over valence s and p orbitals at atom sites near the impurity. From this analysis, it was deduced that 73% of the wave function was on only one of the neighboring silicon atoms (12% s and 88% p), while 9% was located on the nitrogen atom (28% s and 72% p). Stress measurements reveal the character of the orbital to be antibonding between the silicon and the nitrogen. The nitrogen defect has an electronic donor level in the gap, and when the defect loses an electron, the nitrogen presumably goes on center and the defect regains tetrahedral symmetry.

The behavior of nitrogen is distinctly different from that of its neighbors in the Periodic Table: carbon, which remains tetrahedral,[46] and oxygen, which displaces off center in a ⟨100⟩ direction from the tetrahedral site to have a ground-state C_{2v} symmetry.[26,27] The cause of this distortion is a source of some controversy.[16,19–21] The source of the difference in the behavior of these different impurities is an interesting and largely ignored problem. Why nitrogen displaces in a ⟨111⟩ direction and oxygen in a ⟨100⟩ direction is a mystery so far unexplained.

The motive force for the nitrogen distortion becomes immediately apparent within a local bonding picture. Figure 7 schematically depicts the expected electronic configuration about the nitrogen atom in this defect, analogous to the bonding expected for ammonia [see Fig. 4(a)]. The nitrogen atom, as in ammonia, will form three covalent bonds with neighboring silicon atoms (Si_B—Si_D), while the presence of the lone pair of electrons on the nitrogen and the dangling-bond electron on the remaining silicon atom (Si_A) precludes the formation of a fourth bond. The unpaired electron will have some amplitude on the nitrogen atom, but will be antibonding in nature so as to remain orthogonal to the lone-pair orbitals. The nitrogen atom will move off in the $[\bar{1}\,\bar{1}\,\bar{1}]$ direction in order to achieve a more reasonable Si—N bond distance and to reduce the repulsion between the lone pair and the dangling electron. Thus, the principal experimental observations regarding this defect in silicon can be fully accounted for in advance of any calculations.

B. Results: The unrelaxed system

The above qualitative description is confirmed by the results of the cluster perfect-pairing calculations. The wave function of the PP calculation, even in the high-

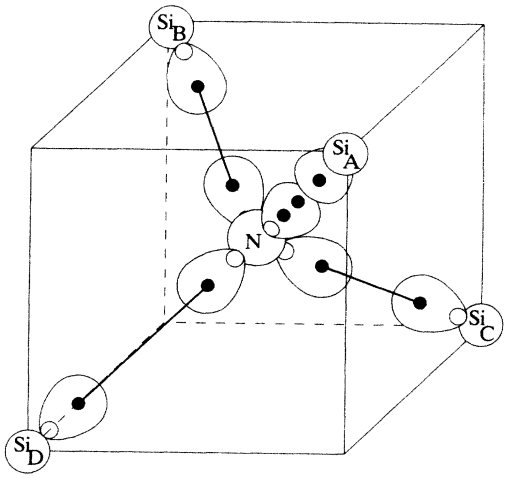

FIG. 7. The schematic depiction of the generalized valence-bond wave function expected for the substitutional nitrogen defect in silicon. The nitrogen will form three equivalent bonds to silicon (Si_B—Si_D) while the fourth bond to the ⟨111⟩ silicon (Si_A) is prevented by the lone pair. The C_{3v} symmetry of this wave function resembles that of ammonia (cf. Fig. 4) and drives the observed C_{3v} distortion.

symmetry T_d geometry, has broken symmetry, hinting at the preferred distortion mode. The symmetry of the wave function is C_{3v} with the axis of symmetry being the [111] axis. The parallel between the bonding here and that of the ammonia system of Fig. 4 is readily apparent. The orbital contour plots of the PP(16/32) wave-function orbitals are exhibited in Fig. 8. Figure 8(c) presents one of three equivalent N—Si bond pairs; C_3 rotations about the [111] axis will bring them into coincidence with one another. A fourth pair of electrons has localized into a lone pair on the nitrogen [Fig. 8(b)], the unpaired electron localizing to occupy the dangling-bond orbital of the remaining silicon atom (Si_A of Fig. 7). The perfect-pairing orbitals of the PP(4/8) wave function about the nitrogen differ negligibly from the corresponding orbitals in the PP(16/32) wave function. The Si—H^x bond electrons have been treated at the HF level, but this does not substantially affect the result in the inner region. The complete removal of perfect-pairing correlation in the calculation results in a HF calculation in which the orbitals have now delocalized throughout the cluster. The theoretical one-electron orbital ordering that has a singly occupied a_1 orbital below an unoccupied t_2 orbital[19–21] is confirmed in this calculation. Besides the energetic difference [the HF wave function is 4.16 eV higher in energy than the PP(16/32) wave function, while the correlation in the PP(4/8) wave function makes it 2.20 eV lower in energy than the HF wave function], what is lost in going from the more general perfect-pairing wave function to the Hartree-Fock wave function is the ability to interpret the orbitals of the wave function in terms of the nature of the bonding (cf. Fig. 7). In the T_d site the qualitative behavior of the nitrogen defect is already anticipated by the perfect-pairing result, in contrast to the lack of any such hint in the HF calculation.

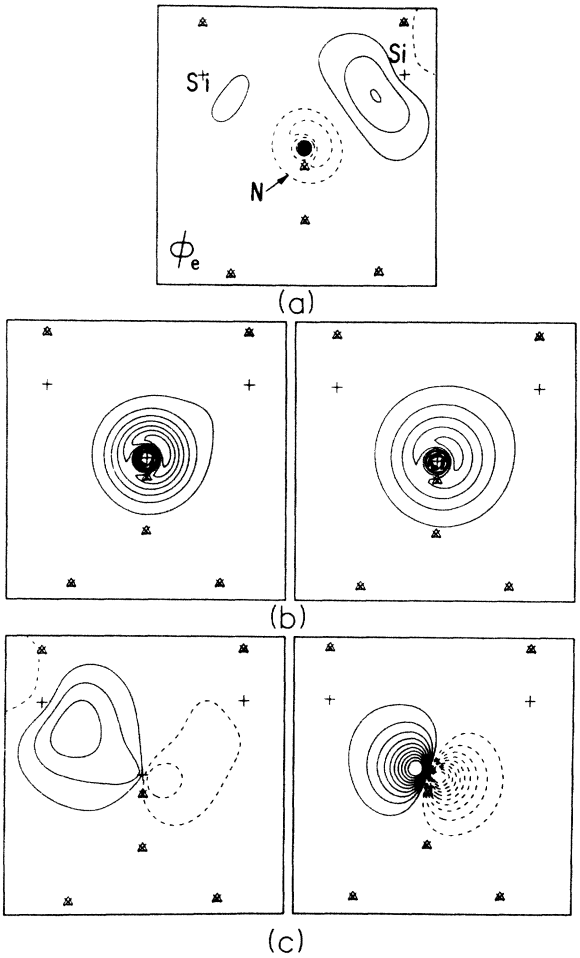

FIG. 8. The orbital contour plots of key orbitals that result from a self-consistent PP(16/23) calculation for the T_d unrelaxed $NSi_4H^x_{12}$ cluster. Notice how clearly the features predicted and schematically represented in Fig. 7 are reproduced in the calculation. (a) The dangling-bond paramagnetic orbital ϕ_e on the ⟨111⟩ silicon (Si_A); (b) the lone pair opposite it, in-out correlated; (c) one of three equivalent Si—N bond pairs (here Si_B—N).

The PP wave function has C_{3v} symmetry, already in accord with the observed behavior. In the rigid tetrahedral cage, however, the total wave function must transform according to some irreducible representation of the T_d point group. The perfect-pairing wave function we have obtained is not unique, as it could be aligned such that the dangling-bond orbital is located on any of the four nearest-neighbor silicon atoms, Si_A—Si_D. Thus, there are four distinct, symmetrically related PP wave functions Ψ_A—Ψ_D, each defined by the location of the dangling-bond orbital. To obtain a total wave function of the proper symmetry, it is necessary to take a linear combination of these symmetrically equivalent PP wave functions to form a R-PP wave function:

$$\Psi_{\text{R-PP}}=\alpha_A\Psi_A+\alpha_B\Psi_B+\alpha_C\Psi_C+\alpha_D\Psi_D\ . \tag{11}$$

In the tetrahedral geometry, this mixing produces one total wave function ($\alpha_A=\alpha_B=\alpha_C=\alpha_D$) of A_1 symmetry,

and three degenerate total wave functions of T_2 symmetry. The R-PP(4/8) calculation for tetrahedral nitrogen finds a ground state of A_1 symmetry that is stabilized by 0.75 eV with respect to the PP(4/8) wave function. The mean-field result also finds an A_1 state below a T_2 state.[20,21] The nature of the many-electron R-PP wave function is quite distinct, though; the character of the bonding about the nitrogen atom remains three bonds and a lone pair. Forcing the PP(4/8) wave function to have four equivalent Si—N bonds and a delocalized a_1 electron (as in the mean-field description), so that it transforms as A_1 in T_d symmetry, significantly raises the energy. Thus the proper description of the many-electron wave function is given by Eq. (11). The correlation effects here are subtle, and very important, calling the efficacy of any simple mean-field approximation into question.

C. Nitrogen displacement in a rigid cage

The wave function derived in the T_d site indicates that the likely mode of distortion, if there is to be any, is a C_{3v} distortion. Acting on this, we consider [111] displacements of the nitrogen atom at three levels of approximation: HF, PP(4/8), and R-PP(4/8). The cluster results described in this section employ the termination distance of 1.50 Å since we do not consider silicon relaxations.[47] Figure 9 presents the energy curves as a function of nitrogen [111] displacement for the three types of wave functions. The HF calculation discloses a very shallow (<0.02 eV) on-center minimum, but with a much deeper minimum of 0.17 eV with the nitrogen displaced 0.52 Å from the tetrahedral position in the $[\bar{1}\,\bar{1}\,\bar{1}]$ direction. This places it only 0.26 Å above the plane of the three silicon (Si_B—Si_D) atoms, giving a Si—N—Si bond angle of 118.6°. The PP(4/8) wave function Ψ_A yields a minimum with the nitrogen atom displaced only 0.24 Å from the tetrahedral site with a depth of 0.16 eV. There is no on-center minimum. If the silicon were truly rigidly clamped at bulk positions, this would represent excellent agreement with the experimentally observed reorientation barrier of 0.11 eV.[25] Denoting the three PP(4/8) wave functions not aligned along the displacement axis by Ψ_B—Ψ_D (defined by the location of the dangling-bond orbital in the wave function), it is apparent that these will no longer be symmetrically equivalent to Ψ_A as the nitrogen is displaced from tetrahedral, though they remain symmetrically related to each other. For a balanced treatment, however, these must be considered for the distorted systems as well as for the T_d-symmetric system in the R-PP wave function. The R-PP(4/8) wave function finds an on-center minimum, albeit a very shallow one. At the PP(4/8) optimal nitrogen displacement of 0.24 Å, the R-PP(4/8) wave-function energy has risen to only 0.06 eV above the energy at the tetrahedrally symmetric site. Therefore our results predict that if the nitrogen was located in a rigid silicon cage the stable geometry would be tetrahedral.

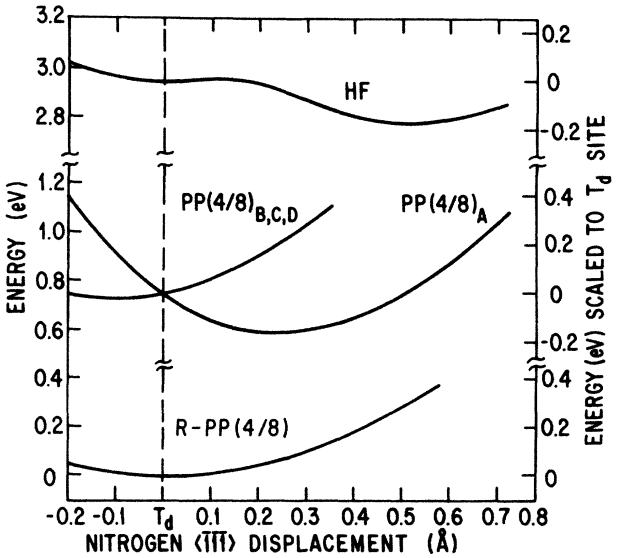

FIG. 9. The potential curves for moving the nitrogen along the [111] direction inside of a frozen unrelaxed silicon cage. The Hartree-Fock result has a shallow on-center minimum and a deeper 0.17-eV minimum at 0.52 Å from the center in the $[\bar{1}\,\bar{1}\,\bar{1}]$ direction. The $PP(4/8)_A$ calculation yields a 0.16-eV minimum at 0.24 Å for the wave function with the lone-pair dangling bond oriented along the [111] axis. $PP(4/8)_B$—$PP(4/8)_D$ represent calculations with the dangling orbital not along the [111] axis of nitrogen displacement. The R-PP(4/8) calculation finds no off-center minimum.

Clearly, the clamping of the silicon atoms in place constitutes an unphysical restriction. It is instructive, however, to root out the source of the differences between the results of the various wave functions. The Hartree-Fock calculation suffers under a pair of difficulties, the most pronounced of these being its inability to describe the stretched bonds that exist here. The unrelaxed N-Si distance is just the bulk Si value of 2.35 Å. This distance is reduced to 2.23 Å for the optimized $[\bar{1}\,\bar{1}\,\bar{1}]$ nitrogen displacement in the Hartree-Fock calculations. One would expect the optimum Si—N bond distance to be ~ 1.73 Å, found to be the equilibrium distance in crystalline Si_3N_4 (Ref. 48) and in the $N(SiH_3)_3$ molecule (Ref. 49). Thus a silicon-nitrogen bond length of 2.23 Å falls in the region where the bonding curve should begin flattening out, but the HF bonding curve continues to rise sharply (cf. Fig. 2, the H_2 curve). The HF wave function therefore overestimates the driving force for shortening these three bonds and the nitrogen is driven planar. This problem is alleviated by the use of the PP(4/8) correlated wave function that allows these bonds to stretch properly. The optimum nitrogen displacement is much smaller for the PP(4/8) calculation and there is no barrier to the displacement. Another deficiency in this HF calculation lies in its inability to describe the C_{3v}→planar→C_{3v} inversion about the nitrogen correctly using this basis set. Using a VDZ basis set, the calculated HF inversion barrier for ammonia is only 0.02 eV, the experimental inversion barrier of 0.25 eV (Ref. 50) being underestimated by 0.23 eV. This suggests that the HF minimum found for the defect is a false one, the minimum being practically fully compensated for by the error in describing the inversion about the nitrogen as it approaches the planar geometry. Including polarization functions in the ammonia calculation yields a more

reasonable barrier[51] and it might be anticipated that including them in the defect calculation might eliminate the HF minimum. Using a PP(4/8) wave function with a VDZ basis for the NH_3 molecule a barrier of 0.08 eV is obtained. However, the necessity to describe the inversion barrier properly is less important for the PP wave function because a much smaller displacement is found [also, the Si—N—Si bond angle only changes from the tetrahedral 109.5° to 114.5° at the PP(4/8) minimum]. With this in mind, polarization functions are not included in the calculation. This underscores, however, the need to exercise extreme care in these geometry optimizations; potentially large errors can be incurred due to basis-set or wave-function[52] limitations.

The primary difference between the PP result and the R-PP result derives from the R-PP being a wave function that transforms according to the correct T_d symmetry, while the individual PP components which constitute the R-PP wave function [Eq. (11)] do not. The coupling between the nitrogen atom and the nearest-neighbor silicon atoms is small due to the long bonds. Hence, the tendency of the PP wave function to induce a displacement of the nitrogen in order to improve the N—Si bonds is overcome by the tendency of the R-PP stabilization to keep the nitrogen on center. When the symmetry is broken, the R-PP stabilization is reduced.

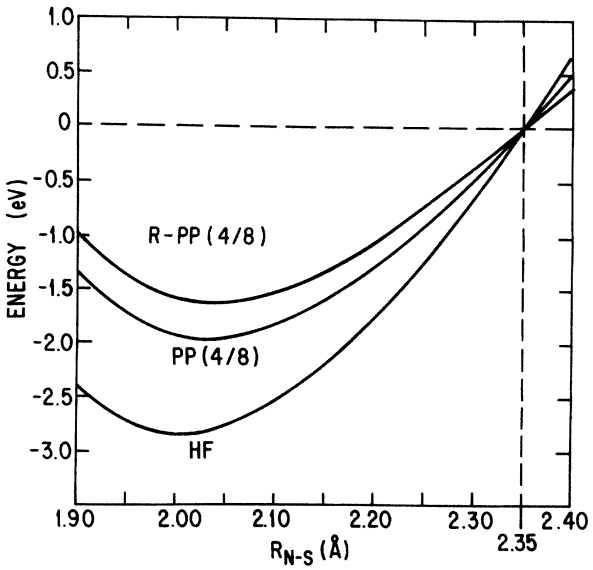

FIG. 10. The effect of the symmetric relaxation of the four silicon atoms radially inwards on the energy of the three types of wave functions. All values scaled to zero at the unrelaxed cluster.

D. Geometry relaxation

1. *Symmetric relaxation of nearest-neighbor silicon atoms*

One anticipates that the silicon atoms should relax inwards from the lattice positions judging from the character of the orbital plots of Fig. 8 and from the fact that the nitrogen atom is much smaller than the silicon atom it replaces. The rigid-cage Si—N bond distance of 2.35 Å is 0.6 Å larger than an equilibrium Si—N bond distance (noted above). The relatively large energy gain obtained upon correlating the inner bonds [HF→PP(4/8)] is another clue that the bonds are very stretched. As pointed out in the H_2 example of Sec. III, increasing correlation energy occurs with increasingly extended bonds [see Fig. 2(b)]. We next consider the radially symmetric relaxation of the silicon atoms about the nitrogen to test this idea. The silicon atoms contract inwards at all levels of approximation, as seen in Fig. 10. The steepest gain is recorded, naturally, for the HF wave function, where the silicon atoms are drawn in 0.34 Å with a corresponding gain of 2.82 eV. The silicon atoms are drawn in somewhat less with the PP(4/8) and R-PP(4/8) wave functions, 0.32 Å, gaining 1.95 and 1.62 eV, respectively, from the unrelaxed cage. The energy differential between the PP(4/8) and HF wave functions has been reduced from 2.20 to 1.33 eV upon inward relaxation. The difference reflects the correlation error made by the HF calculation in attempting to describe the stretched bonds of the unrelaxed system; the radially relaxed new Si-N distance of 2.01 Å is much nearer equilibrium and therefore is relatively better described at the HF level. The orbitals of each of the wave functions, however, have not changed their qualitative forms upon the inward relaxation of the silicon atoms.

2. *Full geometric relaxation of nitrogen and its nearest neighbors*

So far we have not considered symmetry-lowering distortions together with silicon-atom relaxations. We turn now to a discussion of a limited geometry optimization using the PP(4/8) wave function, which investigates distortions of C_{3v} symmetry that the C_{3v} symmetry of the PP wave function and bonding considerations predict to be the symmetry of the optimum distortion. The energy of the PP wave function Ψ_A drops very quickly as the nitrogen and the ⟨111⟩ silicon atom (Si_A of Fig. 7) are separated, clearly indicating the repulsive interaction of the lone pair and the dangling-bond electron. The other basis states of the R-PP(4/8) calculation, the three PP(4/8) wave functions Ψ_B—Ψ_D, became very unstable solutions upon distortion. In comparison to Ψ_A, their energy rises substantially and their contribution to the R-PP(4/8) wave function diminishes as the primary PP wave function Ψ_A becomes a better approximation to the total wave function. The ⟨111⟩ silicon atom returns to an approximately bulk position in the best geometry. The nitrogen moves a total of 0.55 Å off center, yielding a N-Si_A distance of 2.9 Å, reducing the Pauli repulsion between the lone-pair and the dangling-bond electrons greatly. The lone pair and dangling bond are well separated, as a glance at the orbital contour plots of Fig. 11 indicates. The other silicon atoms, Si_B—Si_D, have moved 0.35 Å from their bulk positions and are now within 1.88 Å of the nitrogen atom to which they are bonded (Fig. 11). The energy gained in the perfect-pairing correlation of the inner four pairs is now 1.54 eV as compared to the 2.20 eV of the original unrelaxed geometry. The broken-symmetry PP(4/8) solution is 0.82 eV more stable than

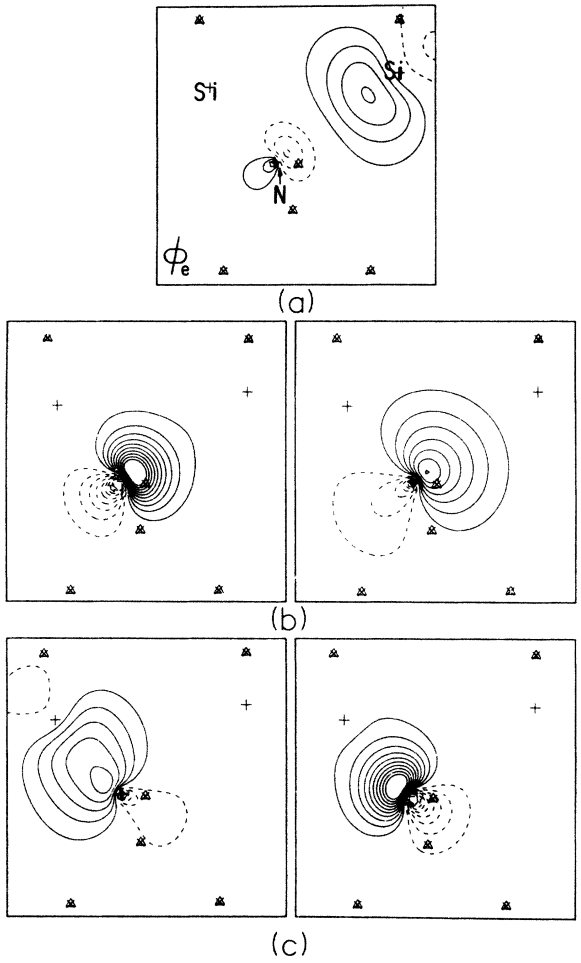

FIG. 11. The PP(16/32) wave-function orbitals at the optimized geometry. The wave function remains qualitatively similar to the PP(16/32) results for the unrelaxed cluster (cf. Fig. 8), where (a), (b), and (c) show the dangling-bond—orbital, nitrogen-lone-pair, and nitrogen-silicon—bond contour plots, respectively.

the equivalent solution for the tetrahedrally relaxed geometry. There is no energy gained from the R-PP calculation at the broken-symmetry geometry, while at the tetrahedral geometry 0.41 eV was gained from mixing in $\Psi_B - \Psi_D$. The net R-PP result is a total lowering upon symmetry breaking of 0.82—0.41=0.41 eV. If the barrier to reorientation were to involve going from one ⟨111⟩ orientation to another through the tetrahedral site geometry, this result would overestimate the observed barrier to reorientation of 0.11 eV.[25] However, it is certainly possible that reorientation takes place through a C_{2v} pathway rather than through the high-symmetry T_d site. In fact, this possibility appears quite reasonable as the T_d pathway involves stretching all three bonds, while the C_{2v} route would involve only the stretching of one bond while keeping the other two relatively constant. The search for a C_{2v} minimum, however, was not attempted here. A further consideration is the fact that the R-PP calculation is not fully-self-consistent, and this would incur a larger error in the symmetric site energy than in the broken-symmetry site energy. For the C_{3v} optimum geometry, the PP(4/8) wave function is an excellent approximation to the R-PP(4/8) and little stabilization energy from mixing in the other PP(4/8) wave-function components is obtained.

The true HF minimum for this model should be well approximated by the HF energy at the optimum PP geometry. Assuming a reorientation through the tetrahedral geometry, the HF reorientation barrier is calculated to be at least 0.7 eV. This is larger than the value obtained for the correlated wave functions and greatly overestimates the observed value.

The removal of an electron from the C_{3v} system allows the fourth bond to form, causing the atoms of the ionized defect to relax and bring the nitrogen on center. The calculated stable geometry for the ionized nitrogen impurity has full tetrahedral symmetry using both the HF and the correlated PP wave functions. Upon recapture of an electron, the neutral defect relaxes back to the neutral C_{3v} ground-state geometry. The energy of the atomic relaxation of the ionized defect to the tetrahedral geometry and the complementary relaxation of the neutralized defect from the tetrahedral to the C_{3v} optimum geometry need not be the same. In fact, the relaxation of the ionized defect to the PP(4/8) optimum T_d geometry ($R_{\text{Si-N}}=2.02$ Å) is calculated to be 1.43 eV, while the relaxation of the neutralized defect returns only 0.41 eV.

The calculated ionization energy for a cluster cannot be directly equated to levels in the fundamental gap in silicon. The calculation does not include the electron affinity of the conduction band with respect to vacuum, estimated from experiment to be $\sim$4.0 eV.[32] Also neglected is the polarization of the lattice in response to the change in charge state. The calculated nitrogen defect cluster-ionization energy of 6.1 eV (including atomic relaxation) does not include these effects. From comparison with other defect calculations which indicate that a shallow-level defect ionization costs 4—5 eV,[53] we can deduce that the nitrogen level in the gap will be deep, most likely closer to the valence-band than to the conduction-band edge. What is unambiguously demonstrated by this calculation is the large charge-state dependence of the atomic relaxation energies. This provides one plausible source of the difficulty in experimentally locating this elusive level. Clearly, extreme care must be taken in the interpretation of experimental data when it is possible for such atomic relaxation energies to exceed the band-gap energy.

E. Hyperfine calculations

Electron paramagnetic resonance provides some of the most detailed knowledge about deep-level defects in semiconductors.[3,54] Fortunately, such information is available for the case of the nitrogen defect, and, in fact, constitutes our major knowledge of this defect. The anisotropic spectrum labeled SL5 that emerges for the neutral substitutional nitrogen in silicon[25] can be described by a simple spin-$\frac{1}{2}$ Hamiltonian:

$$H=\mu_B \mathbf{H}\cdot\overleftrightarrow{g}\cdot\mathbf{S}+\sum_j \mathbf{I}_j\cdot\overleftrightarrow{A}_j\cdot\mathbf{S}\ , \tag{12}$$

with $S=\frac{1}{2}$, $\mathbf{I}_j$ are the nuclear spins, $\mathbf{H}$ is the magnetic field, and μ_B is the Bohr magneton. The components of the hyperfine tensor $\overleftrightarrow{A}_j$ are given by[53]

$$A_{\lambda\gamma}=g_e\mu_B\mu_N(\mu_j/I_j)\left[\left\langle\psi_e\left|\frac{3r_\lambda r_\gamma-\delta_{\lambda\gamma}r^2}{r^5}\right|\psi_e\right\rangle+\frac{8\pi}{3}|\psi_e(0)|^2\delta_{\lambda\gamma}\right], \quad (13)$$

where μ_j is the nuclear magnetic moment and r is the distance with respect to site j. The dominant contributions come from the s and p character of the orbital at a given atomic site, so it is convenient to divide this into two parts: the isotropic part due to the s occupation and the anisotropic part deriving from the p character. In an axially symmetric spectrum, the axial and perpendicular components of the hyperfine tensor are trivially related:

$$A_{j,\text{iso}}=\frac{8\pi g_e}{3}\mu_B\mu_N(\mu_j/I_j)|\psi_e(0)|^2=\frac{A_{j,\parallel}+2A_{j,\perp}}{3}, \quad (14a)$$

$$A_{j,\text{ani}}=\frac{4g_e}{5}\mu_B\mu_N(\mu_j/I_j)\langle r_{j,e}^{-3}\rangle=\frac{A_{j,\parallel}-A_{j,\perp}}{3}. \quad (14b)$$

Conventionally, in the analysis of the experiment for a single paramagnetic electron, it is assumed that the character of the wave function can be described by the single molecular orbital of Eq. (10) and one attempts to fit the parameters η_j^2, α_j^2, and β_j^2 (total amplitude on atom, percent s, and percent p, respectively) with the approximations

$$|\psi_e(0)|^2=|\psi_{j,ns}(0)|^2\eta_j^2\alpha_j^2$$

and

$$\langle r_e^{-3}\rangle=\langle r_{j,np}^{-3}\rangle\eta_j^2\beta_j^2 .$$

The atomic valence orbital values $|\psi_{j,ns}(0)|^2$ and $\langle r_{j,np}^{-3}\rangle$ are taken from results tabulated from Hartree-Fock atomic calculations. With this analysis, it is possible to determine in great detail the character of the paramagnetic orbital. Brower[25] analyzed his data in this manner to determine that the paramagnetic orbital is located 73% on the $\langle 111\rangle$ silicon atom (Si_A of Fig. 7), 12% s and 88% p in character, and 9% (28% s and 72% p) on the nitrogen.

A Mulliken analysis provides the simplest means of comparing the results of the calculations with experiment. For the unrelaxed geometry, the broken-symmetry PP(16/32) solution already exhibits the correct qualitative behavior (see Fig. 8) with 63% of the electron on the silicon (14% s and 86% p), but yields a net negative population on the nitrogen [a deficiency in the Mulliken analysis: this negative population is belied by the obvious amplitude that the orbital has on the nitrogen in the contour plot of Fig. 8(e)]. When the nitrogen is allowed to move, but with the silicon atoms still fixed in place, the electron localizes strongly on the silicon so that 86% of the orbital lies on the silicon atom in a Mulliken analysis for the perfect-pairing wave functions at the optimal nitrogen displacement. Furthermore, this has a Si s-p distribution in good agreement with experiment: $(12\pm2)\%$ s, $(88\pm2)\%$ p. This is a clue that the silicon atom will remain at approximately its bulk position since the s-p balance is very sensitive to the atom location. As the silicon atoms are drawn in symmetrically, the ratio changes, increasing the s character at the expense of p character, so that at a silicon-nitrogen distance of 2.04 Å (inward 0.31 Å) the orbital has 23% s and 77% p character on Si_A. This behavior of a threefold-coordinated silicon atom with a dangling-bond electron is the same when calculated for the dangling orbital on the (111) silicon surface.[33] The optimal location for the $\langle 111\rangle$ silicon atom, as described above, is approximately the bulk position.

Table IV presents the Mulliken analysis of the paramagnetic orbital for the perfect-pairing and Hartree-Fock wave functions in the equilibrium cluster geometry. Once the stretched bonds are relaxed, the HF represents a more satisfactory approximation. This is reflected in how closely the HF paramagnetic orbital mimics the results of the PP calculations. As experimentally observed, the majority of the electron amplitude is in the silicon dangling bond for these calculations and the 15% s/85% p ratio compares favorably with experiment. Unfortunately, the Mulliken analysis still gives a net zero result for the nitrogen population, which is clearly contradicted by the paramagnetic orbital's amplitude on the nitrogen seen in Fig. 11. The problem originates from the character of the orbital on the nitrogen. The atomic valence occupation of the nitrogen atom is $2s^22p^3$ and these orbitals are fully saturated in the defect system by the three bond pairs and the lone-pair electrons. The paramagnetic orbital is reduced to partially occupying the "3s" and "3p" orbitals, a situation that the valence Mulliken analysis cannot handle properly due to the node introduced into the valence region. To remedy this problem and to simultaneously

TABLE IV. Mulliken analysis over paramagnetic orbital from the self-consistent wave function calculated at best geometry with the $NSi_4H^x_{12}$ cluster. Distribution of paramagnetic electron in percent.

Wave function	$\langle 111\rangle$ silicon Total	% s	% p	Nitrogen Total	% s	% p
Expt.	73%	12	88	9%	28	72
PP(16/32)	91.9	14.3	85.7	1.2	~0	100
PP(4/8)	90.1	15.1	84.9	1.1	~0	100
HF	88.8	15.1	84.9	1.1	~0	100

TABLE V. Hyperfine parameters $|\psi(0)|^2$ and $\langle r^{-3}\rangle$ calculated for valence orbitals of isolated silicon and nitrogen atoms. All entries in $10^{24}/cm^3$.

	Si[a]		N	
	$\|\psi_{3s}(0)\|^2$	$\langle r_{3p}^{-3}\rangle$	$\|\psi_{2s}(0)\|^2$	$\langle r_{2p}^{-3}\rangle$
After Brower[b]	25.84	13.68	32.51	20.38
Double zeta[c]	25.58	12.13	32.25	16.39
DZ + Rydberg *sp*	25.60	12.12	32.25	16.40
Si $11s4p$/N $9s5p$	25.16	12.13	30.52	16.39

[a] ^5S state ($s^1x^1y^1z^1$) calculated.
[b] See Ref. 14.
[c] DZ=Si($11s7p/6s4p$) and N($9s5p/4s2p$). See Sec. II and Ref. 25.

gauge the accuracy of the Mulliken analysis on the silicon atom, we treated the core electrons of the ⟨111⟩ silicon explicitly (leaving the other silicon atoms with effective potentials). Using a full double-zeta basis set or better for both this silicon and the nitrogen to assure adequate basis-set flexibility, we calculate these parameters [$|\psi(0)|^2$ and $\langle r^{-3}\rangle$] more directly from the wave function.

For reference, Table V presents the calculated atomic values with the basis sets we used for the atoms. For the nitrogen atoms, the state from which the parameters were calculated was the Hartree-Fock $^4S(1s^22s^22x^12y^12z^1)$ ground state. The reference state used for the silicon atom was the ^5S(core $3s^13x^13y^13z^1$) high-spin state rather than the silicon ground ^3P state; this was done to reflect the nominal sp^3 hybridization of the silicon atom in the lattice. The effect of changing the basis is seen to be small. We can calculate $|\psi(0)|^2$ and $\langle r^{-3}\rangle$ from the wave function, and compare them with the atomic values to obtain proportions of atomic populations or can apply Eq. (14) to calculate the hyperfine terms directly. Table VI contains a summary of results from the calculations. For simplicity of presentation, the calculated values are recorded as percentages of atomic-orbital populations. The first part of the table contains the results from the simple, full double-zeta calculation in the optimum geometry, including both the Mulliken analysis and direct calculation of the occupations. Notably, the results on the silicon atom do not greatly vary, indicating an occupation that is 90% of the atomic occupation for both calculations. The *s-p* proportion of ~14% *s* and ~86% *p* in the Mulliken analysis and ~19% *s* and ~81% *p* in the direct calculation are both in excellent agreement with the experimentally observed 12% *s*/88% *p* ratio. A significant difference between values calculated from Mulliken analyses and those obtained directly from the wave function is noted for the nitrogen atom, however. While the Mulliken analysis suggests a zero occupation, the direct calculation derives a figure that represents ~7% occupation on the nitrogen atom with approximately 20% *s* and

TABLE VI. Hyperfine values for the paramagnetic orbital from self-consistent wave functions. For the nitrogen atom and the ⟨111⟩ silicon atoms, all electrons are considered: for the other silicon atoms effective potentials are used. As described in the text, the results are scaled using values obtained for the valence orbitals of the isolated atoms. Values in parentheses represent results from a Mulliken analysis. Distribution of paramagnetic electron in percent.

Cluster basis set	Wave function	⟨111⟩ silicon Total	⟨111⟩ silicon *s*/*p* proportion	Nitrogen Total	Nitrogen *s*/*p* proportion
Full	PP(16/32)	91.0	17.1/82.9	6.64	20.8/79.2
		(91.8)	(13.7/86.3)	(1.24)	(all *p*)
Double	PP(4/8)	90.3	18.7/81.3	6.02	19.9/80.1
		(90.2)	(14.6/85.4)	(0.96)	(all *p*)
Zeta	HF	88.8	18.7/81.3	7.65	19.8/80.2
		(88.8)	(14.6/85.4)	(2.25)	(all *p*)
Si $11s4p$	PP(16/32)	91.0	17.0/83.0	6.64	20.8/79.2
POL (*d*'s)	PP(16/32)	85.3	19.1/80.9	6.73	21.8/78.2
RYD (*s*,*p*)	PP(16/32)	93.1	21.8/78.2	11.27	13.7/86.3
Extended cluster	PP(16/32)	(88.7)	(13.4/86.6)	6.66	20.4/79.6
⟨111⟩ SiH_3 in 0.1 Å	PP(16/32)	89.7	17.8/82.2	8.33	20.9/79.1
⟨111⟩ Si in 0.1 Å	PP(16/32)	90.3	19.2/80.7	7.46	20.9/79.1
Experiment[a]		73%	12/88	9%	28/72

[a] Reference 14.

80% p, now also in very good agreement with experiment (9%; 28% s and 72% p).

To gauge the effects of some of the approximations of our model, we alter the model slightly in order to investigate the possibilities individually. The wave function used throughout is the PP(16/32) in which all 16 valence pairs are correlated. One of the first possibilities that might come to mind is a deficiency in the basis set. The basis set used so far in the calculations has included neither polarization functions nor Rydberg functions. Furthermore, since the calculation is very sensitive to the wave function very near the nucleus, it might be necessary to have a more flexible basis set than even the DZ basis. The actual basis used does not consist of Slater-type orbitals (STO's), but of Gaussians contracted to mimic STO's, and this could have an effect near the nucleus because of the cusps in the atomic orbitals that are poorly described by the Gaussians. This particular concern is already partially addressed by quoting figures as proportions of the atomic values calculated using an identical basis set, the premise being that any error would scale properly. To determine the possible magnitude of the effect, the 11s Gaussians of the $\langle 111 \rangle$ silicon were completely uncontracted in one calculation. The result, as seen in the table (Si 11s4p), is identical to the result obtained using the contraction. Adding d-type polarization functions (POL) on the $\langle 111 \rangle$ silicon atom and nitrogen atom does reduce the population on the silicon by 6%, but the overall description remains very much the same. Adding Rydberg s and p basis functions (RYD) on the five central atoms also has little effect, mostly noticeable as a slight increase in the amplitude at the nitrogen to 11% (22% s and 78% p). The final result appears quite insensitive to the alteration of the basis set employed here, a very encouraging sign, suggesting that the DZ description is quite adequate.

Another possible source of error can be the limitation imposed on the orbital due to the restricted cluster size. In this instance, most of the paramagnetic orbital amplitude is situated on the $\langle 111 \rangle$ silicon, an atom bonded to three terminators rather than silicon, and it is reasonable to suspect that the electron may be prevented from properly delocalizing onto these sites. To address this issue, we replaced each of the terminators bonded to the $\langle 111 \rangle$ silicon atom with SiH^x_3 moieties. In this extended cluster, the stoichiometry is $NSi_7H^x_{18}$ and has C_{3v} symmetry. The nitrogen atom was described using a full double-zeta basis, but due to computational considerations the $\langle 111 \rangle$ silicon core electrons were replaced by an effective potential. The use of the effective potential on the $\langle 111 \rangle$ silicon has yielded values for the Mulliken analysis very similar to those derived from all-electron calculations (compare Tables IV and VI) for the dangling-bond orbital, so this is not a severe restriction. Upon the self-consistent calculation of the PP(16/32) wave function for the extended cluster, hyperfine parameters calculated for the silicon and the nitrogen atoms do not differ significantly from those obtained using the smaller cluster model (cf. Table VI). The $NSi_4H^x_{12}$ model is clearly sufficient to allow for the delocalization of this electron.

Yet another potential source of error relates to the inability of this model to account for lattice relaxation beyond the first shell with great accuracy. The nitrogen atom induces large displacements from bulk positions in the silicon atoms to which it is bonded. While our terminators do have midely weaker force constants than actual silicon bonds to account for potential lattice relaxation, the 0.35 Å distance that the silicon atoms are calculated to move from bulk positions strains the reliability of this model. In order to assess the potential effect this restriction has on the calculated hyperfine values, the relative positions of the $N(SiH^x_3)_3$ and $\langle 111 \rangle$ SiH^x_3 moieties were varied along the [111] axis. Moving the two moieties toward each other (SiH^x_3 in 0.1 Å) increases the amplitude on the nitrogen atom while decreasing the amplitude on the silicon atom, bringing the results into closer agreement with experiment. Moving the $\langle 111 \rangle$ silicon atom 0.1 Å in along the axis toward the nitrogen atom 0.1 Å has roughly the same effect.

TABLE VII. Direct calculation of the isotropic and anisotropic hyperfine terms using the double-zeta $NSi_5H^x_{12}$ cluster. All terms in 10^{-4} cm^{-1}, obtained from evaluation of Eq. (14).

	$\langle 111 \rangle$ silicon		Nitrogen	
	A_{iso}	A_{ani}	A_{iso}	A_{ani}
Expt.	95.7	18.4	13.10	1.00
Calc.	174.9	19.1	7.09	0.66

The isotropic and anisotropic values obtained without scaling by the calculates atomic values $|\psi(0)|^2$ and $\langle r^{-3} \rangle$ will not be fully reliable due to the inability of the Gaussian basis set to model STO's correctly near the nucleus. Table VII illustrates this, presenting the hyperfine terms calculated without any scaling. This and the atomic values of Table IV seem to suggest that while the amplitude at the nucleus (Fermi contact) for the orbital is reasonably well produced, the overall shape near the nucleus (important for the anisotropic term) is not so well reproduced. Scaling via the atomic-orbital values is therefore appropriate and the resulting general agreement of theory with experiment is very good.

VI. DISCUSSION

A. Nitrogen impurity in silicon

The results of the generalized valence-bond cluster model unambiguously confirm the qualitative picture discussed in Sec. V A using no more than simple chemical and physical concepts. The inclusion of correlation has played a key role in the interpretation of the wave functions, giving the calculations a predictive capability absent in a simpler mean-field methods. The driving force for the C_{3v} distortion has been clearly demonstrated to be due to *local* bonding considerations, i.e., the nitrogen, as elsewhere in nature (e.g., ammonia) attempts to form three good bonds and one lone pair. For the neutral defect, this dictates that the system will have an overall C_{3v} symmetry, with the nitrogen displaced in the $[\bar{1}\,\bar{1}\,\bar{1}]$ direction

from the tetrahedral position to form those three good bonds, while simultaneously relieving the repulsion between the lone-pair and the dangling-bond electrons on the silicon atom. This argument finds support in studying the evolution of the perfect-pairing wave function as one goes from the unrelaxed tetrahedral system, to the relaxed tetrahedral system, to the optimum C_{3v}-symmetry ground-state geometry. The use of the wave function to calculate the hyperfine terms demonstrates that the wave function self-consistently derived within this cluster approximation accurately represents the electronic structure within the local vicinity of the defect. The fact that minor modifications in the model do not significantly affect the results is further testimony that this approach is justified.

We have perhaps pointed out a danger in taking the interpretation of EPR data in terms of proportions of atomic populations too literally. In the example treated here, the amplitude of the paramagnetic electron on the nitrogen does not involve the occupation of the "2s" and "2p" orbitals in terms of which they are analyzed, but involves partial occupation of the "3s" and "3p" orbitals. For a silicon dangling-bond orbital, such an analysis is satisfactory because the electron nominally occupies a valence orbital. This distinction between valence and excited orbitals could, however, have profound implications for conclusions drawn about the degree of delocalization of paramagnetic electrons in other systems, where the amount of occupation on a more distant silicon atom is determined as a proportion of the Si atomic 3s and 3p orbitals. To say that EPR records a value for the hyperfine parameter that amounts to 1% of the atomic valence orbital value on a site is different from saying that 1% of the electron is located there. The "3s" and "3p" orbitals of the silicon atoms in the lattice are already nominally saturated by the valence-band electrons. A further caution must be mentioned about the reference values used in an analysis. The appropriate atomic reference state for silicon is the $sp^3\,{}^5S$ state and not the $s^2p^2\,{}^3P$ ground state.

Finding that the substitutional nitrogen defect is satisfactorily described, we go on to speculate about other systems. Nitrogen's neighbors in the Periodic Table have distinctly different behavior from nitrogen and each other, as already noted. Nitrogen is a single deep donor with C_{3v} symmetry; substitutional oxygen is a single acceptor that resides in a geometry of C_{2v} symmetry. It has been well characterized by infrared spectroscopy,[27] and while the neutral defect has no net spin, the negatively charged defect has a paramagnetic electron and has been studied with EPR.[26] The level has been clearly identified as lying 0.17 eV below that conduction-band edge. Carbon, on the other side of nitrogen, retains the tetrahedral symmetry and exhibits no electrical activity.[46] Within a view point that is grounded in one-electron theories, there is no *a priori* reason to presume that they differ in their behavior when located substitutionally for one of the silicon atoms. When placed in the tetrahedral site, the one-electron wave function for all three impurity systems will be nondegenerate, with the valence orbitals all fully occupied and either 0, 1, or 2 electrons in the highest occupied a_1 orbital. The next step in this line of attack is to determine if such a system should distort, and if so, why, and in which direction. A calculation of a potential curve within the one-electron theories may be capable of finding the correct distortions, but one is often left without a truly satisfying explanation of the cause of the distortion and without any explanation why a particular distortion mode should be preferable to another.

The observed behavior can be accounted for within the conceptual framework that we have described. Figure 12 presents the valence-bond diagrams for the expected behavior of nitrogen neighbors in the Periodic Table when located substitutionally. Consider first the carbon impurity. Carbon fourfold-coordinates (as in methane) and trivially replaces the silicon atom in the lattice [Fig. 12(d)] as in Fig. 12(a), forming the four bonds that the silicon left behind. The defect retains T_d symmetry. The nearest-neighbor silicon atoms are drawn radially in toward the carbon, for the same reasons detailed for the relaxation inwards of those silicon atoms towards the nitrogen impurity. No electrical activity would be expected: there are no available orbitals out of which to eject an electron from, or to capture an electron into, that would result in a level in the gap. The neutral nitrogen defect case has been discussed in detail above. The relationship between the neutral nitrogen and the positive ion state is analogous to that between ammonia NH_3 and the ammonium ion NH_4^+, which is also tetrahedral. In the silicon lattice, the NSi_4^+ defect center is very similar in its bonding characteristics to the carbon-atom impurity.

The behavior of the oxygen "A center" differs dramatically. Atomic oxygen, which has two singly occupied orbitals, can form two bonds just as in the water molecule.

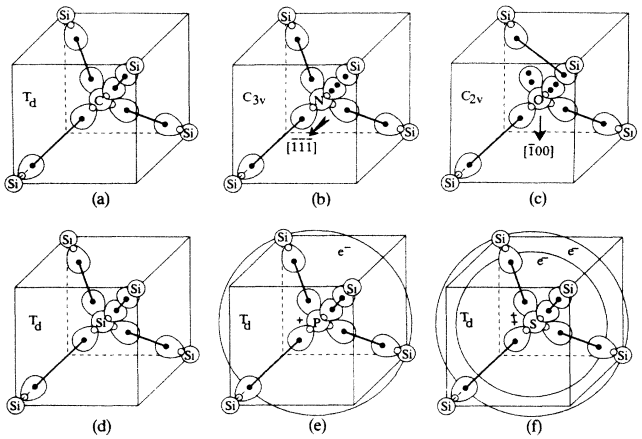

FIG. 12. Schematic representation of the electronic wave function expected for various atoms placed in the silicon site. (a) Carbon, fourfold coordinated, retaining T_d symmetry; (b) nitrogen; threefold coordinated, C_{3v} ground state results; (c) oxygen, bonds to two silicon, with two weekly overlapping silicon dangling orbitals forming tenuous bond, C_{2v} ground state results; (d) silicon; (e) phosphorus, the electron is ejected into a Rydberg-like orbital and four equivalent bonds formed to the neighboring silicon, therefore retaining T_d symmetry; (f) sulfur, both electrons in Rydberg-like orbitals, allowing four equivalent bonds and a T_d ground-state geometry.

To create two strong bonds while simultaneously reducing the repulsion of the two oxygen lone pairs with the dangling orbitals on the silicon, the oxygen strongly displaces in a ⟨100⟩ direction and has a ground-state geometry of C_{2v} symmetry. The two dangling bonds on the silicon atoms weakly overlap and will form a tenuous, very stretched bond. An electron entering this system will enter (in one-electron terms) the antibonding orbital of this bond. Because of symmetry, there will be no isotropic hyperfine component on the oxygen, consistent with EPR data.[26] Furthermore, the oxygen will be rather far removed from this weak Si—Si bond, so that the amplitude of the extra unpaired electron on the oxygen would be very small in any case. Effectively, the electron is in a system that resembles half a silicon vacancy. That the character of this system is very similar to that of the vacancy was noted by Watkins and Corbett.[26] Simple GVB-PP calculations for this system confirm the qualitative picture just described, but a thorough study, such as has been presented for the $Si{:}N_{Si}$ described above, has not yet been performed.

The phosphorus substitutional center is the canonical shallow donor and should be, at best, only poorly described by a cluster as small as the one used here. The spin density is known to extend over 30—40 shells of silicon atoms,[55,56] while the cluster includes but the first two. Conceptually, however, this system poses no more difficult a challenge. Phosphorus remains tetrahedral, unlike the nitrogen with which it is isovalent, because while the nitrogen could distort to form good bonds and reduce the lone-pair repulsion, the P—Si bonds are already near equilibrium due to the comparable orbital sizes of the atoms. Therefore, there is no need to displace the phosphorus atom to strengthen the bonds. Furthermore, the barrier to inversion about the phosphorus is much higher, also negating any significant distortion. The result is that the repulsion of the lone pair and the dangling electron drives the electron out into a Rydberg-like hydrogenic orbital, allowing the formation of a fourth bond, regaining the T_d symmetry of the center. The local configuration is then that depicted in Fig. 12(e), in which the local wave function is approximately described by four equivalent Si—P bonds, with the nominally positive charge on the phosphorus binding the Rydberg-like electron. The situation for sulfur [Fig. 12(f)] would be similar, except that both extra electrons are bound into Rydberg-like states while the sulfur is nominally doubly charged.

The PP calculation for $Si{:}P_{Si}$ is somewhat hampered by the extreme truncation of the paramagnetic orbital, but still does rather well. As in the nitrogen case, there are two types of perfect-pairing wave functions that could conceivably describe this system: the description just offered with four symmetrically equivalent bonds and a Rydberg-like electron or, alternatively, a broken-symmetry solution with three equivalent bonds, a lone pair, and a dangling electron. While for the nitrogen case, the T_d PP wave function was prohibitively higher in energy than the C_{3v} PP wave function, the two possibilities for the phosphorus are separated by <0.1 eV [PP(16/32)], the broken-symmetry solution still being the lower. A R-PP(4/8) calculation finds the symmetric linear combination (A_1 state) of the four equivalent PP(4/8) solutions to be the ground state. Though not attempted, we expect the P atom to remain on center just as for the case of the R-PP result for the nitrogen case in the unrelaxed system (Fig. 10), since in the phosphorus case the driving force is to keep the phosphorus on center, the silicon-phosphorus bond distance being already near equilibrium without any relaxation. Perhaps the source of the discrepancy between theory and experiment for the ground state of the phosphorus, commonly attributed to central-cell effects, is due to just such subtle correlation effects. This illustrates that the situation may be more complex than that of the simple qualitative description outlined above; the true picture may not be amenable to a mean-field description of a single electron above an occupied valence band.

B. Prospects and limitations of the method

It is extremely encouraging that the cluster model developed above serves as a useful tool in the investigation of simple defect systems. The pertinent ground-state bulk properties are faithfully reproduced in this attempt to approximate the local aspects of the bulk wave function of Eq. (8) with the cluster wave function of Eq. (9). The detailed agreement of theory with EPR only serves as further confirmation of the validity of this approach.

Manifestly, there are difficulties within a cluster method. The formal treatment of the host lattice has been traded for the ability to treat the local region of interest in greater detail and in the process develop some conceptual tools useful in the understanding of defect systems. In a sense, all deep-level defect approaches, even the Green's-function methods, treat only a small number of atoms rigorously and treat the presence of the host in some approximate manner. The most glaring problem of the small-cluster approach is the current inability to precisely locate the energy levels of the defect with respect to the band edges. Computationally, the levels can only be inferred, but not precisely calculated. Along this vein, however, even the best current Green's-function approaches can claim a computational precision of only ± 0.5 eV (or the width of the gap) in the calculations.[14] While the cluster approach, in its current state of development, cannot locate these levels, the potential precision with which it can compare to EPR experiments, demonstrated by the nitrogen hyperfine calculations of this study, stands as a challenge to other methods.

In their simulations of the host, the terminators act as a pseudopotential for the host. In principle, this concept could be further refined, so that the approximation of going from the bulk [Eq. (8)] to cluster [Eq. (9)] wave function can be improved. Potential factors left out of the calculation include (a) the response of the more distant lattice sites to the strain about the center of the defect system, (b) the polarization of the lattice in response to a charge disturbance, (c) the location of the band edges, and (d) truncation of the defect wave-function orbitals. The problem of (a) is tempered by a judicious choice in the truncation of the cluster and could be remedied by the use of a Keating-type model[57] to account for the elastic response of the lattice. Polarization effects can be ad-

dressed by some dielectric model. Location of the band edges is a more difficult task since the excited valence-band and conduction-band states are by their very nature delocalized. It could, perhaps, be parametrized, using some cluster reference energy for the band edges. As demonstrated for the nitrogen case, the electronic states for many deep defects will be very localized in nature and it will be possible to rank energies relative to one another. The truncation of the wave-function orbitals that extend greatly beyond the bounds of the first few shells of atoms, such as the phosphorus shallow donor, will pose the largest problem. Conceptually simple, they remain computationally out of reach due to computational limitations. For most deep-level defect systems of interest, the wave function remains dominantly localized, as in the case of the nitrogen. Truncating any small amplitude outside of the cluster should not be energetically significant.

The calculated wave function holds a great deal of information, in the calculation of the hyperfine terms and in elucidating the nature of the electronic structure (i.e., the bonding). The comprehensive study of the direct calculation of the hyperfine parameters as presented here is extremely rare. Comparisons to hyperfine values, if attempted, usually involve using Mulliken populations of a wave function or limit themselves to treating a single site rigorously.[58]

The concepts that we have introduced to describe these defects stand independently of the technical details of the calculations. The ability to predict the qualitative behavior of a defect using simple bonding concepts *without* calculations is a valuable tool, often lost in theoretical studies of defect systems. The clear conceptual picture presented provides relatively simple explanations of the observed behavior of several simple defect systems, explanations not possible within a mean-field approach. Furthermore, this method possesses a natural generalization to the study of defects in amorphous systems where one-electron band states are not even a zeroth-order approximation to the electronic structure.

VII. CONCLUSIONS

The goals of this study were twofold. One was to justify and to demonstrate the utility of using local bonding concepts as a framework within which to discuss and predict defect behavior in semiconductors. The qualitative descriptions presented in a previous work[24] and elaborated on further here illustrate the advantages inherent in such an outlook. The arguments, based totally on local bonding considerations, have proven to be a highly successful tool for understanding defect behavior. A useful feature is the commonality of language when one goes from defects in otherwise crystalline systems to defects in amorphous systems.

The second goal of this study was to demonstrate the viability of the localized bond model as the ansatz for a workable computational scheme. We have demonstrated that including the dominant correlation effects in covalent systems, intrapair correlation, results in wave functions that formally justify the use of the concepts that were used. The approximation chosen, the perfect-pairing form of the generalized valence-bond theory, is shown to be suitable for use in this cluster approach. We provide a new formal justification for the cluster approximation within the strategy of mimicking the local electronic structure of the bulk system, i.e., the local orbitals of Eq. (8) by the electronic orbitals of the cluster wave function of Eq. (9). We found that a specially developed terminating atom can produce just the desired characteristics in the wave function and rigorous tests find that it reproduces the pertinent bulk properties very well.

The use of a small $X\mathrm{Si}_4\mathrm{H}^x_{12}$ cluster was found sufficient to describe a system such as the nitrogen substitutional defect. Keeping the terminators fixed and allowing the nitrogen and its neighboring silicon atoms to adjust, the proper C_{3v} symmetry for the ground state was found to naturally result. Using the calculated wave function directly, an in-depth comparison to the most detailed experimental information about the wave function available, EPR, produced excellent agreement, supporting the validity and accuracy of the cluster model and the type of the wave function used. Unfortunately, in its current state of development, the approach is unable to directly locate the electronic energy level with respect to the band edges. What the calculations do reveal is the extremely large role that atomic relaxations play in the calculation of a level position, anticipating the difficulty associated in experimentally locating this level. The atomic relaxation of the ionized defect from the threefold-coordinated site (optimal for the neutral defect) to the optimal ion tetrahedral geometry involved an energy 0.2 eV larger than the fundamental gap. The complementary relaxation of the neutral defect upon capture of an electron in the tetrahedral geometry to the optimal neutral C_{3v} geometry returned only 0.4 eV, a full 1 eV difference. We have further conclusively demonstrated that, to describe the crucial local relaxations properly, it is necessary to use a theory that has demonstrated its ability to handle a regime where stretched, broken, and reformed bonds are the norm, not the exception. The comparison of the uncorrelated HF results with the perfect-pairing results, which account for the minimum necessary correlation to describe the breaking of a bond, illustrates this point. Strained bonds are the inevitable consequence of the introduction of defects into systems where the neighboring host atoms are constrained by the lattice.

A final point that emerged is a note of caution against drawing conclusions about the degree of delocalization of paramagnetic electrons on the basis of EPR populations derived from using atomic valence orbitals as a reference.

ACKNOWLEDGMENTS

This work was supported in part by the National Science Foundation Material Research Laboratory (MRL) Program under Grant No. DMR-82-16718 at the Laboratory for Research on the Structure of Matter, University of Pennsylvania. The authors are grateful to C. M. Kao for useful discussions and for the use of his R-GVB program, to S. H. Lamson for invaluable assistance in computations on a Cray computer, and to R. C. Tatar for helpful comments and a critical reading of the manuscript.

[1]Reviews of theoretical studies of defects in semiconductors can be found in S. T. Pantelides, Rev. Mod. Phys. **50**, 797 (1978); M. Jaros, Adv. Phys. **29**, 409 (1980); R. C. Newman, Rep. Prog. Phys. **45**, 1163 (1982).

[2]W. Kohn, in *Solid State Physics,* edited by F. Seitz and D. Turnbull (Academic, New York, 1957), Vol. 5.

[3]J. W. Corbett, R. L. Kleinhenz, and You Zhi-pu, in *Defect Complexes in Semiconductor Structures,* Vol. 175 of *Lecture Notes in Physics,* edited by J. Giber (Springer-Verlag, Berlin, 1983).

[4]A. R. Williams, P. J. Feibelman, and N. D. Lang, Phys. Rev. B **26**, 5433 (1982).

[5]G. Baraff, M. Schlüter, and G. Allan, Phys. Rev. Lett. **50**, 739 (1983).

[6]R. Car, P. J. Kelly, A. Oshiyama, and S. T. Pantelides, Phys. Rev. Lett. **52**, 1814 (1984).

[7]W. Kohn and L. J. Sham, Phys. Rev. **140**, A1133 (1965).

[8]P. Hohenberg and W. Kohn, Phys. Rev. **136**, B864 (1964).

[9]M. S. Hybertsen and S. G. Louie, Phys. Rev. B **30**, 5777 (1984).

[10]M. T. Yin and M. L. Cohen, Phys. Rev. B **26**, 5668 (1982).

[11]D. R. Hamann, Phys. Rev. Lett. **42**, 662 (1979).

[12]G. B. Bachelet and N. E. Christensen, Phys. Rev. B **31**, 879 (1985).

[13]J. P. Perdew and M. Levy, Phys. Rev. Lett. **51**, 1884 (1983); L. J. Sham and M. Schlüter, *ibid.* **51**, 1888 (1983); Phys. Rev. B **32**, 3883 (1985); C. S. Wang and W. E. Pickett, Phys. Rev. Lett. **51**, 597 (1983); A. E. Carlsson, Phys. Rev. B **31**, 5178 (1985).

[14]G. Baraff and M. Schlüter, Phys. Rev. B **30**, 3460 (1984).

[15]C. A. Coulson and M. J. Kearsley, Proc. R. Soc. London, Ser. A **241**, 433 (1957).

[16]R. P. Messmer and G. D. Watkins, Phys. Rev. B **7**, 2568 (1973).

[17]W. V. Smith, P. P. Sorokin, I. L. Gelles, and G. J. Lasker, Phys. Rev. **115**, 1546 (1959).

[18]H. A. Jahn and E. Teller, Proc. R. Soc. London, Ser. A **161**, 220 (1937).

[19]M. Lannoo, Phys. Rev. B **25**, 2987 (1982).

[20]G. B. Bachelet, G. A. Baraff, and M. Schlüter, Phys. Rev. B **24**, 4736 (1981).

[21]G. G. DeLeo, W. B. Fowler, and G. D. Watkins, Phys. Rev. B **29**, 3193 (1984), and references therein.

[22]G. T. Surratt and W. A. Goddard III, Phys. Rev. B **18**, 2831 (1978).

[23]L. Pauling, *Nature of the Chemical Bond,* 3rd ed. (Cornell University Press, Ithaca, 1960).

[24]R. P. Messmer and P. A. Schultz, Solid State Commun. **52**, 563 (1984); R. P. Messmer, J. Non-Cryst. Solids **75**, 285 (1985).

[25]K. L. Brower, Phys. Rev. Lett. **44**, 1627 (1980); Phys. Rev. B **26**, 6040 (1982).

[26]G. D. Watkins and J. W. Corbett, Phys. Rev. **121**, 1001 (1961).

[27]J. W. Corbett, G. D. Watkins, R. M. Chrenko, and R. S. McDonald, Phys. Rev. **121**, 1015 (1961).

[28]R. A. Bair, W. A. Goddard III, A. F. Voter, A. K. Rappe, L. G. Yaffe, F. W. Bobrowicz, W. R. Wadt, P. J. Hay, W. J. Hunt, GVB2P5 program (unpublished); R. A. Bair, Ph.D. thesis Cal Tech, 1980; F. W. Bobrowicz and W. A. Goddard III, in *Modern Theoretical Chemistry: Methods of Electronic Structure Theory,* edited by H. F. Schaefer III (Plenum, New York, 1977), Vol. 3, pp. 79—127; W. J. Hunt, P. J. Hay, and W. A. Goddard III, J. Chem. Phys. **57**, 738 (1972).

[29]A. K. Rappe, T. A. Smedley, and W. A. Goddard III, J. Phys. Chem. **85**, 1662 (1981).

[30]A. F. Voter and W. A. Goddard III, Chem. Phys. **57**, 253 (1981).

[31](a) S. Huzinaga, J. Chem. Phys. **42**, 1293 (1965); (b) T. H. Dunning, Jr. and P. J. Hay, in *Modern Theoretical Chemistry: Methods of Electronic Structure Theory,* Ref. 28, pp. 1—27; (c) T. H. Dunning, Jr., J. Chem. Phys. **53**, 2823 (1970).

[32]A. Redondo, W. A. Goddard III, C. A. Swarts, and T. C. McGill, J. Vac. Sci. Technol. **19**, 498 (1981).

[33]A. Redondo, W. A. Goddard III, T. C. McGill, and G. T. Surratt, Solid State Commun. **20**, 733 (1976).

[34]A. Redondo and W. A. Goddard III, J. Vac. Sci. Technol. **21**, 344 (1982).

[35]W. A. Goddard III, J. J. Barton, A. Redondo, and T. C. McGill, J. Vac. Sci. Technol. **15**, 1274 (1978).

[36]D. D. Wagner *et al.*, J. Phys. Chem. Ref. Data **11**, Suppl. 2 (1982).

[37]That is, to obtain the Si—Si bond energy from X_2H_6, we must subtract out X—H bond energies calculated from XH_4. The X—H bond energy may differ slightly in the two cases.

[38]G. Herzberg, *Electronic Spectra and Electronic Structure of Polyatomic Molecules,* Vol. III of *Molecular Spectra and Molecular Structure* (Van Nostrand, New York, 1966).

[39]C. Kittel, *Introduction to Solid State Physics,* 5th ed. (Wiley, New York, 1976).

[40]J. C. Slater, *Quantum Theory of Molecules and Solids* (McGraw-Hill, New York, 1963), Vol. 1.

[41]T. H. Upton, J. Phys. Chem. **87**, 3865 (1983).

[42]P. A. Schultz and R. P. Messmer (unpublished).

[43]R. S. Mulliken, J. Chem. Phys. **23**, 1833 (1955).

[44]Using GAUSSIAN80 computer program: J. S. Binkley, R. Whiteside, R. Krishnan, R. Seeger, H. B. Schlegel, D. J. DeFrees, S. Topiol, L. R. Kahn, and J. A. Pople, Quantum Chemistry Program Exchange **13**, 406 (1981).

[45]*Landolt-Börnstein: Numerical Data and Functional Relationships in Science and Technology,* New Series (Springer-Verlag, New York, 1982), Vol. III/17a.

[46]R. C. Newman and J. B. Willis, J. Phys. Chem. Solids **26**, 373 (1965).

[47]Cluster termination of 1.73-Å derived relative energies upon nitrogen displacement similar to the results of the 1.50-Å termination.

[48]O. Borgen and H. M. Seip, Acta Chem. Scand. **15**, 1789 (1961); R. Marchand, Y. Laurent, J. Lang, and M. Th. Le. Bihan, Acta Crystallogr. B **25**, 2157 (1969).

[49]*Landolt-Börnstein: Numerical Data and Functional Relationships in Science and Technology,* New Series, Ref. 45, Vol. II/7.

[50]J. D. Swalen and J. A. Ibers, J. Chem. Phys. **36**, 1914 (1962).

[51]R. M. Stevens, J. Chem. Phys. **61**, 2086 (1974).

[52]The PP wave function does not take into account possible spin recouplings among the PP orbitals, necessary for the correct dissociation of multiple bonds, e.g., N_2. In principle, spin recoupling of the orbitals about the nitrogen atom could play a role in the results due to the stretched nature of the three Si—N bonds. CI calculations that allow for a fully general doublet spin function among the nine orbitals of the interior of the cluster indicate that the energy stabilization with respect to the PP energy is almost constant in all geometries. Therefore this refinement of the wave function is not necessary for a physically meaningful discussion of the nitrogen impurity problem and no further discussion of this more general wave function is given here.

[53]P. A. Schultz and R. P. Messmer, unpublished results.

[54]G. Lancaster, *Electron Spin Resonance in Semiconductors* (Plenum, New York, 1967).
[55]G. Feher, Phys. Rev. **114**, 1219 (1959).
[56]E. B. Hale and R. L. Mieher, Phys. Rev. **184**, 739 (1969); **184**, 751 (1969).
[57]P. N. Keating, Phys. Rev. **145**, 637 (1966); R. M. Martin, Phys. Rev. B **1**, 4005 (1970).
[58]H. Katayama-Yoshida and A. Zunger, Phys. Rev. B **31**, 8317 (1985).